Received: xxx **Accepted:** xxx **Published:** xxx.
DOI: 10.30473/coam.2026.77231.1394
Volume xxx, Issue xxx, p.p. 1-23: xxx
Research Article

Control and Optimization in Applied Mathematics - COAM

Open Access

An Explicit Finite Difference Scheme for Time-Fractional Stochastic Traveling Wave Equations Driven by Multiplicative White Noise

Priti Mojad[1], Babasaheb Gavhane[2], Shrikisan Gaikwad[3], Kalyanrao Takale[4], Chetan Shirore[5] ✉

[1]Department of Mathematics, New Arts Commerce and Science College, Ahmednagar, affiliated to Savitribai Phule Pune University, Pune, India
[2]Department of Mathematics, K. J. Somaiya College of Arts, Commerce and Science, Kopargaon, India
[3]Department of Mathematics, New Arts Commerce and Science College, Ahmednagar, India
[4]Department of Computer Science, Jaykranti College of Computer Science and Management, Pune, India
[5]Department of Mathematics, K.R.T. Arts, B.H. Commerce and A.M. Science College, Nashik, India

✉ **Correspondence:**
Chetan Shirore
E-mail:
chetanshirore@kthmcollege.ac.in

How to Cite
Mojad, P., Gavhane, B., Gaikwad, S., Takale, K., Shirore, C. (2027). "An explicit finite difference scheme for time-fractional stochastic traveling wave equations driven by multiplicative white noise". *Control and Optimization in Applied Mathematics*, X(x), 1–23. https://doi.org/10.30473/coam.2026.77231.1394

Abstract. This work addresses the numerical approximation of the time-fractional stochastic traveling wave equation (TFSTWE) with a Caputo fractional derivative of order $\alpha \in (1,2]$ driven by multiplicative space-time white noise. An explicit finite difference method (FDM) is constructed by discretizing the space domain. For the first time step, a mean-square stability bound and an error estimate of order $\mathcal{O}(\Delta t^{2-\alpha} + \Delta x^2)$ are derived under a restriction on Δt that depends explicitly on Δx, the diffusion coefficient $\mathcal{K}$, and the fractional order α, while the noise intensity σ enters the mean-square growth constant; stability and convergence at later time levels are supported numerically. Comprehensive numerical experiments demonstrate the effectiveness and reliability of the proposed method, and the Python programming language is used to plot the approximate mean solution profiles in two and three dimensions. The outcomes confirm the suitability of the method for accurately solving TFSTWEs under stochastic perturbations and support the theoretical analysis.

Keywords. Explicit difference approximation, Fractional derivatives, Mean square method, Multiplicative white noise.

MSC. 60H15; 26A33; 65M06.

1 Introduction

Fractional stochastic calculus offers a natural framework for capturing randomness and memory effects in complex systems. Combining fractional calculus with stochastic processes such as Brownian motion and white noise makes it possible to describe accurately systems that exhibit long-term dependence and uncertainty [4]. Fractional stochastic differential equations (FSDEs) incorporate both memory and uncertainty effects, and they work well precisely where classical differential equations fall short in capturing uncertainty and long memory. When white noise is present, FSDEs are generally interpreted in infinite-dimensional probability spaces and are often formulated using Caputo derivatives [2]. These equations have found applications in several fields: in biology, to describe disease propagation and population dynamics under stochastic impacts [20, 23]; in finance, to capture long-memory features of market dynamics [1, 11]; and in physics, to model turbulence and thermal memory effects [7, 21].

To solve FSDEs, a variety of numerical techniques have been developed, such as Adomian decomposition, spectral methods, finite element methods, and finite difference methods [12, 14]. Finite difference schemes stand out for their simplicity, flexibility, and ease of implementation on structured grids. Explicit finite difference method (FDM) schemes are computationally simple and easy to implement, although they come with a conditional stability requirement. They also suit real-world FSDE applications well, since they can be readily adapted to higher-dimensional problems and to random disturbances [24]. Moghaddam et al. [14] reviewed in detail the development of FDM, spectral, and meshless approaches for fractional stochastic partial differential equations, including both additive and multiplicative white noise cases.

Other researchers have proposed various discretization approaches for FSDEs. Singh et al. [19] introduced a cubic B-spline-based collocation technique that solves the fractional diffusion-wave equation with higher precision and lower computational cost. Chukwuyem et al. [3] addressed time-fractional stochastic wave equations using the Crank–Nicolson finite element method (CNFEM), which offers a stable and reliable numerical framework. By combining finite difference schemes with Python-based visualizations, Ghode et al. [6] developed a computational framework for solving time-fractional wave equations. Singh and Mehra [18] proposed difference schemes for stochastic space-fractional diffusion equations with additive space–time white noise using the Wong–Zakai approximation and a shifted Grünwald–Letnikov formula. Hoult and Yan [8] proposed a numerical scheme for Caputo-type stochastic fractional differential equations with integrated multiplicative noise, approximating the noise by a piecewise constant function. Li et al. [10] developed a finite difference method for Caputo generalized time-fractional diffusion equations, extending the L1 scheme in time and using central differences in space. Mojad et al. [15] employed a Crank–Nicolson finite difference scheme for space–time fractional stochastic traveling wave equations with additive white noise, where the noise is independent of the solution. Unlike this additive case, multiplicative noise couples directly with the solution, which introduces additional challenges and motivates the present work.

In the present work, we employ an explicit FDM to solve the TFSTWE driven by multiplicative space-time white noise. The TFSTWE considered here, together with its initial and boundary conditions, is given by

$$\begin{aligned}
{}^{C}\mathscr{D}_t^{\alpha}\mathcal{V}(x,t) &= \mathcal{K}^2\,\frac{\partial^2\mathcal{V}(x,t)}{\partial x^2} + \sigma\,\mathcal{V}(x,t)\,\dot{\mathcal{W}}(x,t), \\
&\qquad 0 < x \le \mathcal{L},\ 0 < t \le \mathcal{T},\ 1 < \alpha \le 2, && \text{(1a)}\\
\mathcal{V}(x,0) &= \Psi_1(x), && \text{(1b)}\\
\mathcal{V}_t(x,0) &= \Psi_2(x), && \text{(1c)}\\
\mathcal{V}(0,t) &= 0, && \text{(1d)}\\
\mathcal{V}(\mathcal{L},t) &= 0. && \text{(1e)}
\end{aligned}$$

The term ${}^{C}\mathscr{D}_t^{\alpha}\mathcal{V}(x,t)$ denotes the Caputo fractional derivative of order $\alpha \in (1,2]$ of the stochastic process $\mathcal{V}(x,t)$. The functions $\Psi_1(x)$ and $\Psi_2(x)$ are known initial data, assumed to be bounded and continuous on $[0,\mathcal{L}]$, which ensures the existence of a unique solution to the model (1). Here, σ denotes the noise amplitude, and $\mathcal{L}$, $\mathcal{K}$, and $\mathcal{T}$ are positive constants. The term $\dot{\mathcal{W}}(x,t)$ is a space-time white noise defined on a filtered probability space $(\Omega, \mathcal{F}, \{\mathcal{F}_t\}_{t\ge 0}, \mathbb{P})$, where Ω is the sample space of all possible outcomes, $\mathcal{F}$ is the complete σ-algebra of events, and the filtration $\{\mathcal{F}_t\}_{t\ge 0}$ satisfies the usual conditions of right-continuity and completeness. Throughout this paper, $\dot{\mathcal{W}}(x,t)$ is a generalized Gaussian process with zero mean and the delta-correlated covariance structure

$$\mathbb{E}\big[\dot{\mathcal{W}}(x,t)\,\dot{\mathcal{W}}(s,y)\big] = \delta(x-s)\,\delta(t-y),$$

where $\delta(\cdot)$ denotes the Dirac delta function. This is the distributional derivative of the Brownian sheet and corresponds to space-time white noise.

The remainder of this paper is organized as follows. Section 2 introduces the essential definitions and lemmas from fractional stochastic calculus. Section 3 describes the proposed numerical scheme in detail. The mean-square stability and the error of the first time step are analyzed in Sections 4 and 5, respectively, together with a discussion of the difficulties at later time levels. Section 6 presents a numerical example implemented in Python, in which the behavior of the solution is illustrated graphically to show how the dynamics of the system are affected by both random perturbations and the fractional order. The results are discussed in Section 7, and Section 8 concludes the paper.

2 Preliminaries

This section reviews the essential definitions and lemmas from fractional stochastic calculus that are used in the subsequent analysis.

Definition 1. Let w be a continuous real-valued function defined on $[0,\infty)$. For a fractional order $\alpha > 0$ such that $n-1 < \alpha \leq n$ with $n \in \mathbb{N}$, the Caputo fractional derivative [9] is defined by

$$\mathcal{D}_t^{\alpha} w(t) := \begin{cases} \dfrac{1}{\Gamma(n-\alpha)} \displaystyle\int_0^t (t-\zeta)^{n-\alpha-1}\, w^{(n)}(\zeta)\, d\zeta, & \text{if } n-1 < \alpha < n, \\ w^{(n)}(t), & \text{if } \alpha = n \in \mathbb{N}, \end{cases}$$

where $w^{(n)}$ denotes the classical derivative of order n of w. The Euler gamma function $\Gamma(\cdot)$ is defined for $p > 0$ by

$$\Gamma(p) := \int_0^{\infty} e^{-x} x^{p-1}\, dx.$$

Definition 2. A stochastic difference scheme is said to be stable in the mean-square sense [16] if there exist positive constants ϵ and δ and non-negative constants λ and v such that

$$\mathbb{E}\left\|\mathcal{U}^{n+1}\right\|_{\infty}^{2} \leq \lambda\, e^{vt}\, \mathbb{E}\left\|\mathcal{U}^{0}\right\|_{\infty}^{2}$$

for all $t = (n+1)\Delta t$, where $\mathbb{E}[\cdot]$ is the mathematical expectation operator on the probability space $(\Omega, \mathcal{F}, \mathbb{P})$. The time step Δt and the space step Δx must satisfy $0 < \Delta x \leq \epsilon$ and $0 < \Delta t \leq \delta$. A difference scheme is called unconditionally stable if no restriction is imposed on the relation between Δx and Δt; otherwise, it is called conditionally stable.

Definition 3. A stochastic difference scheme $\mathcal{L}_i^m \mathcal{S}_i^m = \mathcal{G}_i^m$ that approximates a stochastic differential equation (SDE) $\mathcal{L}\mathcal{S} = \mathcal{G}$ at time $t = (m+1)\Delta t$ is said to be convergent in the mean-square sense [13] if

$$\mathbb{E}\left\|\mathcal{S}_i^m - \mathcal{S}\right\|_{\infty}^{2} \to 0 \quad \text{as } i\Delta x \to x,\ m\Delta t \to t,\ \Delta x \to 0,\ \Delta t \to 0.$$

Lemma 1 (Sun and Wu [22])**.** Let $b_j = (j+1)^{2-\alpha} - j^{2-\alpha}$ for $j = 1, 2, \ldots$ and $\alpha > 0$. Then

1. $b_j > 0$ (positivity);
2. $b_j > b_{j+1}$ (monotonically decreasing);
3. $b_{j+1} - b_j < b_j - b_{j-1}$ (convexity).

Lemma 2 (Young's inequality)**.** For real numbers x, y and any $\epsilon > 0$,

$$(x+y)^2 \leq (1+\epsilon)x^2 + \left(1 + \frac{1}{\epsilon}\right)y^2.$$

Proof. By Young's inequality [17], $x^{\nu}y^{1-\nu} \leq \nu x + (1-\nu)y$ for $x, y > 0$ and $0 \leq \nu \leq 1$. Setting $\nu = \frac{1}{2}$ gives $\sqrt{xy} \leq \frac{x+y}{2}$. Substituting $x \to \epsilon x^2$ and $y \to y^2/\epsilon$ yields $|xy| \leq \frac{\epsilon}{2}x^2 + \frac{1}{2\epsilon}y^2$. Hence

$$(x+y)^2 = x^2 + 2xy + y^2 \leq x^2 + 2|xy| + y^2 \leq (1+\epsilon)x^2 + \left(1 + \frac{1}{\epsilon}\right)y^2. \qquad \square$$

Lemma 3 (Jensen's inequality)**.** Let $w_1, w_2, \ldots, w_m \geq 0$ be weights satisfying $\sum_{j=1}^{m} w_j = 1$, and let $x_1, x_2, \ldots, x_m$ be real numbers. Then

$$\left(\sum_{j=1}^{m} w_j\, x_j\right)^2 \leq \sum_{j=1}^{m} w_j\, x_j^2.$$

Proof. By Jensen's inequality [5], for any convex function f,

$$f\left(\sum_{j=1}^{m} w_j\, x_j\right) \leq \sum_{j=1}^{m} w_j\, f(x_j).$$

Since $f(x) = x^2$ is convex, the result follows immediately. $\square$

3 Numerical Scheme

This section presents the explicit difference approximation used to solve the TFSTWE. To develop the numerical scheme for the proposed model (1), we use the following notation. Let $\mathcal{C} = \{t_n = n\Delta t \mid \Delta t = \mathcal{T}/\mathcal{M},\ n = 0, 1, 2, \ldots, \mathcal{M}\}$ be a set of uniformly distributed points in the interval $[0, \mathcal{T}]$. Likewise, let $\mathcal{D} = \{x_i = i\Delta x \mid \Delta x = \mathcal{L}/\mathcal{N},\ i = 0, 1, 2, \ldots, \mathcal{N}\}$ be a set of uniformly distributed points in the interval $[0, \mathcal{L}]$. The quantity $\mathcal{V}_i^n$ denotes the numerical approximation of the exact solution $\mathcal{V}(x_i, t_n)$ at the mesh point (x_i, t_n).

3.1 Approximation in Time

According to Definition 1, ${}^{C}\mathscr{D}_t^{\alpha}\mathcal{V}(x,t)$ can be written as

$${}^{C}\mathscr{D}_t^{\alpha}\mathcal{V}(x,t) = \begin{cases} \dfrac{1}{\Gamma(2-\alpha)} \displaystyle\int_0^t (t-s)^{1-\alpha} \dfrac{\partial^2 \mathcal{V}(x,s)}{\partial s^2}\, ds, & 1 < \alpha < 2,\ x > 0, \\[2ex] \dfrac{\partial^2 \mathcal{V}(x,t)}{\partial t^2}, & \alpha = 2. \end{cases}$$

At the mesh points (x_i, t_n), $i = 1, 2, \ldots, \mathcal{N}-1$ and $n = 1, 2, \ldots, \mathcal{M}-1$, the time-fractional derivative for $1 < \alpha < 2$ is

$$ {}^{C}\mathscr{D}_t^{\alpha}\mathcal{V}(x_i,t_n) = \frac{1}{\Gamma(2-\alpha)} \int_0^{t_n} (t_n - s)^{1-\alpha} \frac{\partial^2 \mathcal{V}(x_i,s)}{\partial s^2}\, ds. $$

Using the substitution property $\int_0^a f(x)\,dx = \int_0^a f(a-x)\,dx$, which holds for any continuous function f defined on $[0,a]$, and splitting the integration interval into the subintervals $[t_j, t_{j+1}]$, we obtain

$$ \begin{aligned} {}^{C}\mathscr{D}_t^{\alpha}\mathcal{V}(x_i,t_n) &= \frac{1}{\Gamma(2-\alpha)} \int_0^{t_n} s^{1-\alpha} \frac{\partial^2 \mathcal{V}(x_i,t_n-s)}{\partial s^2}\, ds \\ &= \frac{1}{\Gamma(2-\alpha)} \sum_{j=0}^{n-1} \int_{t_j}^{t_{j+1}} s^{1-\alpha} \frac{\partial^2 \mathcal{V}(x_i,t_n-s)}{\partial s^2}\, ds \\ &= \frac{1}{\Gamma(2-\alpha)} \sum_{j=0}^{n-1} \int_{t_j}^{t_{j+1}} s^{1-\alpha} \\ &\quad \times \Big(\frac{\mathcal{V}(x_i,t_n-t_{j+1}) + \mathcal{V}(x_i,t_n-t_{j-1}) - 2\mathcal{V}(x_i,t_n-t_j)}{\Delta t^2} \\ &\qquad + \mathcal{O}(\Delta t^{2-\alpha}) \Big) ds \\ &= \frac{1}{\Gamma(2-\alpha)} \sum_{j=0}^{n-1} \Big(\frac{\mathcal{V}(x_i,t_n-t_{j-1}) + \mathcal{V}(x_i,t_n-t_{j+1}) - 2\mathcal{V}(x_i,t_n-t_j)}{\Delta t^2} \\ &\quad + \mathcal{O}(\Delta t^{2-\alpha}) \Big) \\ &\quad \times \Big(\frac{s^{2-\alpha}}{2-\alpha} \Big)_{t_j}^{t_{j+1}} \\ &= \frac{1}{\Gamma(2-\alpha)} \sum_{j=0}^{n-1} \Big(\frac{\mathcal{V}_i^{n+1-j} + \mathcal{V}_i^{n-1-j} - 2\mathcal{V}_i^{n-j}}{\Delta t^2} \\ &\quad + \mathcal{O}(\Delta t^{2-\alpha}) \Big) \\ &\quad \times \Big(\frac{t_{j+1}^{2-\alpha} - t_j^{2-\alpha}}{2-\alpha} \Big) \\ &= \frac{1}{\Gamma(2-\alpha)} \sum_{j=0}^{n-1} \Big(\frac{\mathcal{V}_i^{n+1-j} + \mathcal{V}_i^{n-1-j} - 2\mathcal{V}_i^{n-j}}{\Delta t^2} \\ &\quad + \mathcal{O}(\Delta t^{2-\alpha}) \Big) \\ &\quad \times \Big(\frac{((j+1)\Delta t)^{2-\alpha} - (j\Delta t)^{2-\alpha}}{2-\alpha} \Big) \\ &= \frac{(\Delta t)^{2-\alpha}}{(2-\alpha)\,\Gamma(2-\alpha)} \sum_{j=0}^{n-1} \Big(\frac{\mathcal{V}_i^{n+1-j} + \mathcal{V}_i^{n-1-j} - 2\mathcal{V}_i^{n-j}}{\Delta t^2} \\ &\quad + \mathcal{O}(\Delta t^{2-\alpha}) \Big) \\ &\quad \times \big((j+1)^{2-\alpha} - j^{2-\alpha} \big) \end{aligned} $$

$$
\begin{aligned}
&= \frac{(\Delta t)^{-\alpha}}{\Gamma(3-\alpha)} \sum_{j=0}^{n-1} \big(\mathcal{V}_i^{n+1-j} + \mathcal{V}_i^{n-1-j} - 2\mathcal{V}_i^{n-j}\big)\big((j+1)^{2-\alpha} - j^{2-\alpha}\big) \\
&\quad + \frac{(\Delta t)^{2-\alpha}\,\mathcal{O}(\Delta t^{2-\alpha})}{\Gamma(3-\alpha)} \sum_{j=0}^{n-1} \big((j+1)^{2-\alpha} - j^{2-\alpha}\big) \\
&= \frac{(\Delta t)^{-\alpha}}{\Gamma(3-\alpha)} \sum_{j=0}^{n-1} \big(\mathcal{V}_i^{n+1-j} + \mathcal{V}_i^{n-1-j} - 2\mathcal{V}_i^{n-j}\big)\big((j+1)^{2-\alpha} - j^{2-\alpha}\big) \\
&\quad + \frac{(n\Delta t)^{2-\alpha}\,\mathcal{O}(\Delta t^{2-\alpha})}{\Gamma(3-\alpha)}.
\end{aligned}
$$

Clearly, if $n\Delta t < \infty$, then $(n\Delta t)^{2-\alpha}\,\mathcal{O}(\Delta t^{2-\alpha})/\Gamma(3-\alpha) = \mathcal{O}(\Delta t^{2-\alpha})$. Therefore, the Caputo fractional derivative of order $1 < \alpha < 2$ is approximated, with an error of order $\mathcal{O}(\Delta t^{2-\alpha})$, by

$$
{}^{C}\mathscr{D}_t^{\alpha}\mathcal{V}(x_i, t_n) = \frac{(\Delta t)^{-\alpha}}{\Gamma(3-\alpha)} \sum_{j=0}^{n-1} b_j \big(\mathcal{V}_i^{n+1-j} + \mathcal{V}_i^{n-1-j} - 2\mathcal{V}_i^{n-j}\big), \tag{2}
$$

where $b_j = (j+1)^{2-\alpha} - j^{2-\alpha}$.

3.2 Approximation in Space

At the mesh points (x_i, t_n), $i = 1, 2, \ldots, \mathcal{N} - 1$ and $n = 1, 2, \ldots, \mathcal{M} - 1$, the second-order space derivative is approximated by the central difference

$$
\frac{\partial^2 \mathcal{V}(x_i, t_n)}{\partial x^2} = \frac{\mathcal{V}_{i+1}^n + \mathcal{V}_{i-1}^n - 2\mathcal{V}_i^n}{(\Delta x)^2} + \mathcal{O}\big((\Delta x)^2\big). \tag{3}
$$

3.3 Approximation of the Noise Term

To simulate the stochastic system numerically, we employ the Brownian sheet $\mathcal{W}(x,t)$ over the domain $[0, \mathcal{L}] \times [0, \mathcal{T}]$. Following Hoult and Yan [8], a two-dimensional Brownian sheet satisfies the following properties.

1. *Boundary values:* $\mathcal{W}(x, 0) = \mathcal{W}(0, t) = 0$ for all $x \in [0, \mathcal{L}]$ and $t \in [0, \mathcal{T}]$.
2. *Gaussian increments:* For any rectangle $\mathcal{R} = [x_i, x_{i+1}] \times [t_n, t_{n+1}]$, the rectangular increment

$$
\Delta \mathcal{W}(x_i, t_n) = \mathcal{W}(x_{i+1}, t_{n+1}) - \mathcal{W}(x_i, t_{n+1}) - \mathcal{W}(x_{i+1}, t_n) + \mathcal{W}(x_i, t_n),
$$

is normally distributed with mean zero and variance $\Delta x\, \Delta t$, that is, $\Delta \mathcal{W} \sim \mathcal{N}(0, \Delta x\, \Delta t)$.

3. *Independent increments:* Increments over disjoint rectangles are independent.

The space-time white noise $\dot{\mathcal{W}}(x,t)$ is formally related to the Brownian sheet through the mixed partial derivative $\dot{\mathcal{W}}(x,t) = \partial^2 \mathcal{W}(x,t)/\partial x\, \partial t$. On a regular grid with time step Δt and space step Δx, the noise term at each grid point (x_i, t_n) is approximated as

$$\begin{aligned} \dot{\mathcal{W}}(x_i, t_n) &\approx \frac{\Delta \mathcal{W}}{\Delta x\, \Delta t} \approx \frac{\mathcal{N}(0, \Delta x\, \Delta t)}{\Delta x\, \Delta t} \\ &\approx \frac{\sqrt{\Delta x\, \Delta t}\, \mathcal{N}(0,1)}{\Delta x\, \Delta t} \approx \frac{\mathcal{X}_i^n}{\sqrt{\Delta x\, \Delta t}}, \end{aligned} \tag{4}$$

where $\mathcal{X}_i^n \sim \mathcal{N}(0,1)$ are independent and identically distributed (i.i.d.) Gaussian random variables with zero mean and unit variance.

3.4 Scheme Formulation for the Given Model

Combining the approximations (2), (3), and (4) derived in Sections 3.1–3.3, the numerical approximation of the TFSTWE (1a) takes the form

$$\begin{aligned} &\frac{(\Delta t)^{-\alpha}}{\Gamma(3-\alpha)} \sum_{j=0}^{n-1} b_j \big(\mathcal{V}_i^{n+1-j} + \mathcal{V}_i^{n-1-j} - 2\mathcal{V}_i^{n-j}\big) \\ &\qquad = \mathcal{K}^2\, \frac{\mathcal{V}_{i+1}^n + \mathcal{V}_{i-1}^n - 2\mathcal{V}_i^n}{(\Delta x)^2} + \sigma\, \mathcal{V}_i^n\, \frac{\mathcal{X}_i^n}{\sqrt{\Delta x\, \Delta t}}, \\ &\sum_{j=0}^{n-1} b_j \big(\mathcal{V}_i^{n+1-j} + \mathcal{V}_i^{n-1-j} - 2\mathcal{V}_i^{n-j}\big) \\ &\qquad = \frac{\mathcal{K}^2\, \Gamma(3-\alpha)}{(\Delta t)^{-\alpha}}\, \frac{\mathcal{V}_{i+1}^n + \mathcal{V}_{i-1}^n - 2\mathcal{V}_i^n}{(\Delta x)^2} + \frac{\Gamma(3-\alpha)\, \sigma}{(\Delta t)^{-\alpha}}\, \mathcal{V}_i^n\, \frac{\mathcal{X}_i^n}{\sqrt{\Delta x\, \Delta t}}, \\ &\sum_{j=0}^{n-1} b_j \big(\mathcal{V}_i^{n+1-j} + \mathcal{V}_i^{n-1-j} - 2\mathcal{V}_i^{n-j}\big) \\ &\qquad = \frac{\mathcal{K}^2\, \Gamma(3-\alpha)}{(\Delta t)^{-\alpha} (\Delta x)^2} \big(\mathcal{V}_{i+1}^n + \mathcal{V}_{i-1}^n - 2\mathcal{V}_i^n\big) + \frac{\sigma\, \Gamma(3-\alpha)}{(\Delta t)^{0.5-\alpha} (\Delta x)^{0.5}}\, \mathcal{V}_i^n\, \mathcal{X}_i^n, \\ &\sum_{j=0}^{n-1} b_j \big(\mathcal{V}_i^{n+1-j} + \mathcal{V}_i^{n-1-j} - 2\mathcal{V}_i^{n-j}\big) \\ &\qquad = \frac{\mathcal{K}^2\, \Gamma(3-\alpha) (\Delta t)^{\alpha}}{(\Delta x)^2} \big(\mathcal{V}_{i+1}^n + \mathcal{V}_{i-1}^n - 2\mathcal{V}_i^n\big) + \frac{\sigma\, \Gamma(3-\alpha) (\Delta t)^{\alpha-0.5}}{(\Delta x)^{0.5}}\, \mathcal{V}_i^n\, \mathcal{X}_i^n. \end{aligned}$$

Separating the term $j = 0$ (recall that $b_0 = 1$) from the sum gives

$$\begin{aligned} \mathcal{V}_i^{n+1} + \mathcal{V}_i^{n-1} - 2\mathcal{V}_i^n + \sum_{j=1}^{n-1} b_j \big(\mathcal{V}_i^{n+1-j} + \mathcal{V}_i^{n-1-j} - 2\mathcal{V}_i^{n-j}\big) \\ = a\big[\mathcal{V}_{i+1}^n + \mathcal{V}_{i-1}^n - 2\mathcal{V}_i^n\big] + c\, \mathcal{V}_i^n \mathcal{X}_i^n, \end{aligned} \tag{5}$$

where

$$a=\frac{\mathcal{K}^2\,\Gamma(3-\alpha)(\Delta t)^{\alpha}}{(\Delta x)^2},\qquad c=\frac{\sigma\,\Gamma(3-\alpha)(\Delta t)^{\alpha-0.5}}{(\Delta x)^{0.5}},$$
$$b_j=(j+1)^{2-\alpha}-j^{2-\alpha}, \tag{6}$$

and $\mathcal{X}_i^n\sim\mathcal{N}(0,1)$.

The initial conditions (1b) and (1c) are approximated as

$$\mathcal{V}_i^0=\Psi_1(x_i),\qquad i=0,1,2,\dots,\mathcal{N}, \tag{7}$$
$$\mathcal{V}_i^{-1}=\mathcal{V}_i^1-2\,\Delta t\,\Psi_2(x_i),\qquad i=0,1,2,\dots,\mathcal{N}, \tag{8}$$

and the boundary conditions (1d) and (1e) take the form

$$\mathcal{V}_0^n=0,\qquad n=0,1,2,\dots,\mathcal{M}, \tag{9}$$
$$\mathcal{V}_{\mathcal{N}}^n=0,\qquad n=0,1,2,\dots,\mathcal{M}. \tag{10}$$

For $n=0$, Equation (5) reduces to

$$\begin{aligned}\mathcal{V}_i^1+\mathcal{V}_i^{-1}-2\mathcal{V}_i^0&=a\big(\mathcal{V}_{i+1}^0+\mathcal{V}_{i-1}^0-2\mathcal{V}_i^0\big)+c\,\mathcal{V}_i^0\mathcal{X}_i^0,\\ \mathcal{V}_i^1+\big(\mathcal{V}_i^1-2\,\Delta t\,\Psi_2(x_i)\big)-2\mathcal{V}_i^0&=a\big(\mathcal{V}_{i+1}^0+\mathcal{V}_{i-1}^0-2\mathcal{V}_i^0\big)+c\,\mathcal{V}_i^0\mathcal{X}_i^0,\\ \mathcal{V}_i^1&=\frac{a}{2}\,\mathcal{V}_{i-1}^0+\frac{a}{2}\,\mathcal{V}_{i+1}^0+(1-a)\,\mathcal{V}_i^0+\Delta t\,\Psi_2(x_i)+\frac{c}{2}\,\mathcal{V}_i^0\mathcal{X}_i^0,\end{aligned}$$

where (8) has been used in the second line. The complete discretization of the TFSTWE is therefore given by

$$\mathcal{V}_i^1=\frac{a}{2}\,\mathcal{V}_{i-1}^0+\frac{a}{2}\,\mathcal{V}_{i+1}^0+(1-a)\,\mathcal{V}_i^0+\Delta t\,\Psi_2(x_i)+\frac{c}{2}\,\mathcal{V}_i^0\mathcal{X}_i^0,\qquad n=0, \tag{11}$$

and, for $n\geq 1$,

$$\begin{aligned}\mathcal{V}_i^{n+1}&=a\,\mathcal{V}_{i-1}^n+a\,\mathcal{V}_{i+1}^n+(2-2a-b_1)\,\mathcal{V}_i^n+(2b_1-b_2-1)\,\mathcal{V}_i^{n-1}\\ &\quad-\sum_{j=2}^{n-2}(b_{j-1}+b_{j+1}-2b_j)\,\mathcal{V}_i^{n-j}+(2b_{n-1}-b_{n-2})\,\mathcal{V}_i^1-b_{n-1}\,\mathcal{V}_i^0+c\,\mathcal{V}_i^n\mathcal{X}_i^n.\end{aligned} \tag{12}$$

3.5 Matrix Representation of the Derived Scheme

Let

$$\mathcal{V}^n=\begin{bmatrix}\mathcal{V}_1^n\\ \mathcal{V}_2^n\\ \vdots\\ \mathcal{V}_{\mathcal{N}-1}^n\end{bmatrix},\qquad \mathcal{X}^n=\begin{bmatrix}\mathcal{X}_1^n\\ \mathcal{X}_2^n\\ \vdots\\ \mathcal{X}_{\mathcal{N}-1}^n\end{bmatrix},$$

$$\mathcal{H} = \begin{bmatrix} \Delta t\, \Psi_2(x_1) \\ \Delta t\, \Psi_2(x_2) \\ \vdots \\ \Delta t\, \Psi_2(x_{\mathcal{N}-1}) \end{bmatrix},$$

and let $\mathcal{I}$ denote the identity matrix of order $(\mathcal{N}-1) \times (\mathcal{N}-1)$. The product $\mathcal{V}^n \mathcal{X}^n$ below is understood componentwise. The complete discretized TFSTWE, given by (11) and (12), can then be written in matrix form as

$$\mathcal{V}^1 = \mathcal{Q}_1 \mathcal{V}^0 + \mathcal{H} + \frac{c}{2}\, \mathcal{V}^0 \mathcal{X}^0, \qquad n = 0, \tag{13}$$

and, for $n \geq 1$,

$$\begin{aligned} \mathcal{V}^{n+1} &= \mathcal{Q}_2 \mathcal{V}^n + (2b_1 - b_2 - 1)\, \mathcal{V}^{n-1} - \sum_{j=2}^{n-2} (b_{j+1} + b_{j-1} - 2b_j)\, \mathcal{V}^{n-j} \\ &\quad + (2b_{n-1} - b_{n-2})\, \mathcal{V}^1 - b_{n-1} \mathcal{V}^0 + c\, \mathcal{V}^n \mathcal{X}^n, \end{aligned} \tag{14}$$

where $\mathcal{Q}_1$ and $\mathcal{Q}_2$ are matrices of order $(\mathcal{N}-1) \times (\mathcal{N}-1)$ with entries

$$\mathcal{Q}_1 = (r_{ij}), \quad r_{ij} = \begin{cases} 1 - a, & j = i, \\ a/2, & j = i - 1, \\ a/2, & j = i + 1, \\ 0, & \text{otherwise}, \end{cases}$$

$$\mathcal{Q}_2 = (s_{ij}), \quad s_{ij} = \begin{cases} 2 - 2a - b_1, & j = i, \\ a, & j = i - 1, \\ a, & j = i + 1, \\ 0, & \text{otherwise}. \end{cases}$$

4 Stability Analysis

This section analyzes the mean-square behavior of the proposed scheme. The analysis is carried out for the first time step, where all weights of the scheme are non-negative under the restriction on Δt; the difficulty at later time levels is explained in Remark 1.

Proposition 1 (One-step mean-square bound)**.** Suppose that Δx and Δt satisfy the restriction

$$\Delta t \leq \left[\frac{(\Delta x)^2 (3 - 2^{2-\alpha})}{2\, \mathcal{K}^2\, \Gamma(3 - \alpha)} \right]^{1/\alpha}. \tag{15}$$

Then the first step (11) of the explicit finite difference scheme for the TFSTWE (1) satisfies

$$\mathbb{E}\left\|\mathcal{V}^1\right\|_\infty^2 \le (1+\lambda\Delta t)\,\mathbb{E}\left\|\mathcal{V}^0\right\|_\infty^2 + 2\big(\Delta t+\Delta t^2\big)\left\|\Psi_2\right\|_\infty^2, \tag{16}$$

where

$$\lambda = 1 + \frac{\sigma^2\Gamma(3-\alpha)^2(\Delta t)^{2\alpha-2}}{\Delta x} + \frac{\sigma^2\Gamma(3-\alpha)^2(\Delta t)^{2\alpha-3}}{\Delta x}, \tag{17}$$

$\mathbb{E}\left\|\mathcal{V}^n\right\|_\infty^2 := \sup_{1\le i\le\mathcal{N}-1}\mathbb{E}\left|\mathcal{V}_i^n\right|^2$, and $\left\|\Psi_2\right\|_\infty := \sup_{1\le i\le\mathcal{N}-1}\left|\Psi_2(x_i)\right|$.

Proof. Set $\mathcal{S}_i := \frac{a}{2}\,\mathcal{V}_{i-1}^0 + \frac{a}{2}\,\mathcal{V}_{i+1}^0 + (1-a)\,\mathcal{V}_i^0$. By Equation (11),

$$\mathcal{V}_i^1 = \mathcal{S}_i + \frac{c}{2}\,\mathcal{V}_i^0\mathcal{X}_i^0 + \Delta t\,\Psi_2(x_i).$$

Applying Lemma 2 with $\epsilon = \Delta t$ to the decomposition $x = \mathcal{S}_i$ and $y = \frac{c}{2}\,\mathcal{V}_i^0\mathcal{X}_i^0 + \Delta t\,\Psi_2(x_i)$, and then the elementary inequality $(y_1+y_2)^2 \le 2y_1^2 + 2y_2^2$, we obtain

$$\begin{aligned}\left|\mathcal{V}_i^1\right|^2 &\le (1+\Delta t)\left|\mathcal{S}_i\right|^2 + \left(1+\frac{1}{\Delta t}\right)\left|\frac{c}{2}\,\mathcal{V}_i^0\mathcal{X}_i^0 + \Delta t\,\Psi_2(x_i)\right|^2\\ &\le (1+\Delta t)\left|\mathcal{S}_i\right|^2 + \frac{1}{2}\left(1+\frac{1}{\Delta t}\right)c^2\left|\mathcal{V}_i^0\mathcal{X}_i^0\right|^2\\ &\quad + 2\left(1+\frac{1}{\Delta t}\right)(\Delta t)^2\left|\Psi_2(x_i)\right|^2. \end{aligned}\tag{18}$$

The coefficients $a/2$, $a/2$, and $1-a$ of $\mathcal{S}_i$ sum to exactly 1, so applying Jensen's inequality (Lemma 3) requires them to be non-negative, which imposes the restriction $1-a\ge 0$, that is,

$$\Delta x \ge \mathcal{K}\sqrt{\Gamma(3-\alpha)}\,(\Delta t)^{\alpha/2}. \tag{19}$$

This condition is implied by (15), because $(3-2^{2-\alpha})/2 \le 1$ for $\alpha\in(1,2]$. Under it,

$$\left|\mathcal{S}_i\right|^2 \le \frac{a}{2}\left|\mathcal{V}_{i-1}^0\right|^2 + \frac{a}{2}\left|\mathcal{V}_{i+1}^0\right|^2 + (1-a)\left|\mathcal{V}_i^0\right|^2.$$

Taking expectations and suprema, and using $\mathbb{E}\left|\mathcal{X}_i^0\right|^2 = 1$ together with the independence of $\mathcal{X}_i^0$ from the deterministic initial data, we obtain

$$\sup_{1\le i\le\mathcal{N}-1}\mathbb{E}\left|\mathcal{V}_i^1\right|^2 \le$$

$$\left[(1+\Delta t) + \frac{1}{2}\left(1+\frac{1}{\Delta t}\right)c^2\right]\sup_{1\le i\le\mathcal{N}-1}\mathbb{E}\left|\mathcal{V}_i^0\right|^2 + 2\big(\Delta t+\Delta t^2\big)\sup_{1\le i\le\mathcal{N}-1}\left|\Psi_2(x_i)\right|^2,$$

$$\mathbb{E}\left\|\mathcal{V}^1\right\|_\infty^2 \le \left[1+\Delta t\left(1+\frac{c^2}{2\Delta t}+\frac{c^2}{2\Delta t^2}\right)\right]\mathbb{E}\left\|\mathcal{V}^0\right\|_\infty^2 + 2\big(\Delta t+\Delta t^2\big)\left\|\Psi_2\right\|_\infty^2.$$

Since

$$c^2/\Delta t = \sigma^2\Gamma(3-\alpha)^2(\Delta t)^{2\alpha-2}/\Delta x,$$

and

$$c^2/\Delta t^2 = \sigma^2\Gamma(3-\alpha)^2(\Delta t)^{2\alpha-3}/\Delta x,$$

the bracket is bounded by $1+\lambda\Delta t$, which gives (16). □

Remark 1. For $n \geq 1$, the general step (12) contains the weight $-b_{n-1} < 0$ and, in general, the weight $2b_{n-1} - b_{n-2}$, whose sign is not covered by Lemma 1. Consequently, Jensen's inequality (Lemma 3) cannot be applied to the general step, and the bounds required by Definitions 2 and 3 for all time levels are not established here. Stability over all time levels is supported numerically (Figures 1 and 2 and Table 1) and remains an open problem for an energy-type analysis.

Remark 2. If a bound with the factor $1 + \lambda\Delta t$ held at every time level, it would give $(1 + \lambda\Delta t)^n \leq e^{\lambda n \Delta t} \leq e^{\lambda \mathcal{T}}$, which is uniform in the mesh only if λ remains bounded. Under the restriction (15) alone, λ is in general unbounded as $\Delta x \to 0$; in particular, $\lambda\Delta t \to 0$ is guaranteed only when $\alpha > 4/3$. For $3/2 < \alpha \leq 2$, λ is bounded under the additional restriction

$$\Delta t^{2\alpha-3} \leq K_0 \, \Delta x, \tag{20}$$

with a fixed constant $K_0 > 0$, in which case $\lambda \leq 1 + \sigma^2 \Gamma(3-\alpha)^2 K_0 (1 + \mathcal{T})$. For $\alpha = 2$, condition (20) follows from (15). For $1 < \alpha \leq 3/2$, no such uniform bound is available, and any full-time estimate would hold for each fixed mesh only.

5 Convergence Analysis

In this section, we discuss the consistency of the scheme and the error at the first time step. Convergence over all time levels requires a stability estimate for the general step, as explained in Remark 1.

Proposition 2 (One-step error estimate)**.** Let $\widehat{\mathcal{V}}_i^n$ and $\mathcal{V}_i^n$ denote the exact and approximate solutions of the TFSTWE (1) at the mesh point (x_i, t_n), respectively, and let $\mathcal{E}_i^n = \widehat{\mathcal{V}}_i^n - \mathcal{V}_i^n$. Then the error of the first step (11) of the explicit finite difference scheme satisfies

$$\mathbb{E}\,\big\|\mathcal{E}^1\big\|_\infty^2 = \mathcal{O}\big((\Delta x)^2 + \Delta t^{2-\alpha}\big)^2,$$

where $\mathbb{E}\,\|\mathcal{E}^n\|_\infty^2 := \sup_{1 \leq i \leq \mathcal{N}-1} \mathbb{E}\,|\mathcal{E}_i^n|^2$.

Proof. Let $\mathcal{T}_i^n$ denote the local truncation error at time level n for $1 \leq i \leq \mathcal{N} - 1$. By the consistency of the approximations (2), (3), and (4), the local truncation errors are of order $\mathcal{O}\big((\Delta x)^2 + \Delta t^{2-\alpha}\big)$ in the mean-square sense. From Equations (11) and (12) we have, for $n = 0$,

$$\begin{aligned} \mathcal{T}_i^1 &= \widehat{\mathcal{V}}_i^1 - \frac{a}{2}\,\widehat{\mathcal{V}}_{i-1}^0 - \frac{a}{2}\,\widehat{\mathcal{V}}_{i+1}^0 - (1-a)\,\widehat{\mathcal{V}}_i^0 - \Delta t\,\Psi_2(x_i) - \frac{c}{2}\,\widehat{\mathcal{V}}_i^0 \mathcal{X}_i^0 \\ &= \mathcal{O}\big((\Delta x)^2 + \Delta t^{2-\alpha}\big), \end{aligned} \tag{21}$$

and, for $n \geq 1$,

$$
\begin{aligned}
\mathcal{T}_i^{n+1} &= \widehat{\mathcal{V}}_i^{n+1} - a\,\widehat{\mathcal{V}}_{i-1}^{n} - a\,\widehat{\mathcal{V}}_{i+1}^{n} - (2-2a-b_1)\,\widehat{\mathcal{V}}_i^{n} - (2b_1-b_2-1)\,\widehat{\mathcal{V}}_i^{n-1} \\
&\quad + \sum_{j=2}^{n-2}(b_{j-1}+b_{j+1}-2b_j)\,\widehat{\mathcal{V}}_i^{n-j} - (2b_{n-1}-b_{n-2})\,\widehat{\mathcal{V}}_i^{1} + b_{n-1}\,\widehat{\mathcal{V}}_i^{0} - c\,\widehat{\mathcal{V}}_i^{n}\mathcal{X}_i^{n} \\
&= \mathcal{O}\big((\Delta x)^2 + \Delta t^{2-\alpha}\big).
\end{aligned} \tag{22}
$$

Subtracting the scheme (11) from (21) gives

$$
\mathcal{E}_i^1 = \frac{a}{2}\,\mathcal{E}_{i-1}^0 + \frac{a}{2}\,\mathcal{E}_{i+1}^0 + (1-a)\,\mathcal{E}_i^0 + \frac{c}{2}\,\mathcal{E}_i^0\mathcal{X}_i^0 + \mathcal{T}_i^1.
$$

For the exact initial condition, $\widehat{\mathcal{V}}_i^0 = \mathcal{V}_i^0$, and hence $\mathcal{E}_i^0 = 0$ for all i. Therefore $\mathcal{E}_i^1 = \mathcal{T}_i^1$, and

$$
\mathbb{E}\left\|\mathcal{E}^1\right\|_\infty^2 = \sup_{1\le i\le \mathcal{N}-1}\mathbb{E}\left|\mathcal{T}_i^1\right|^2 = \mathcal{O}\big((\Delta x)^2 + \Delta t^{2-\alpha}\big)^2. \qquad \square
$$

Remark 3. For $n \ge 1$, the error equation obtained by subtracting (12) from (22) contains the same negative weights as the general step. A mean-square error bound over all time levels, as required by Definition 3, therefore follows only from a stability estimate for the general step, which is not established here (see Remark 1). The observed second-order behavior for $\alpha = 2$ in Table 1 is numerical evidence for such a bound.

6 Numerical Experiments

In this section, the numerical experiments were carried out using 1000 Monte Carlo realizations to approximate the mean solution. All simulations were implemented in Python using NumPy, with the random number generator seed fixed at `np.random.seed(0)` to ensure full reproducibility of the reported results.

Example 1. Consider the TFSTWE with multiplicative space-time white noise and the following initial and boundary conditions:

$$
\begin{aligned}
&{}^{C}\mathscr{D}_t^{\alpha}\mathcal{V}(x,t) = \mathcal{K}^2\,\frac{\partial^2\mathcal{V}(x,t)}{\partial x^2} + \sigma\,\mathcal{V}(x,t)\,\dot{\mathcal{W}}(x,t), && (x,t)\in[0,1]\times[0,1],\ 1<\alpha\le 2,\\
&\mathcal{V}(x,0) = \sin(5\pi x) + 2\sin(7\pi x), && 0<x\le 1,\\
&\mathcal{V}_t(x,0) = 0, && 0<x\le 1,\\
&\mathcal{V}(0,t) = 0, && 0<t\le 1,\\
&\mathcal{V}(1,t) = 0, && 0<t\le 1.
\end{aligned}
$$

When $\alpha = 2$ and $\sigma = 0$, the exact solution of the governing equation in Example 1 is [6]

$$
\mathcal{V}(x,t) = \sin(5\pi x)\cos(5\pi\mathcal{K}t) + 2\sin(7\pi x)\cos(7\pi\mathcal{K}t). \tag{23}
$$

The numerical results are shown in Figures 1–5 and Table 1 and are discussed in Section 7.

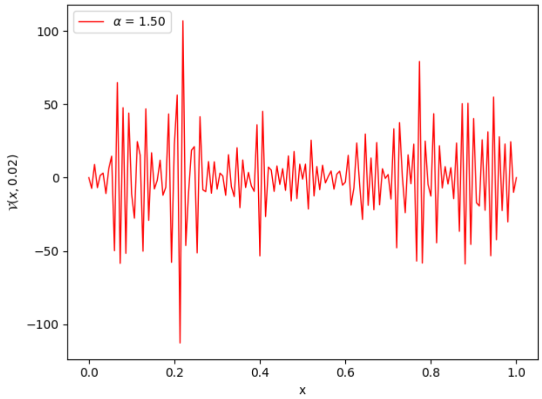

Figure 1: Unstable numerical solution of the TFSTWE for $\alpha = 1.5$ at time $t = 0.02$.

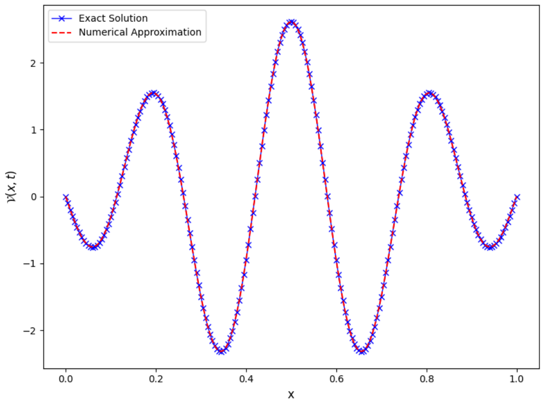

Figure 2: Comparison of the exact solution (23) and the numerical solution of the TFSTWE for $\alpha = 2$, $\sigma = 0$, and $\mathcal{K} = 1$.

Table 1: Global MSE and empirical convergence order $p = \frac{1}{2}\log_2\left(\mathrm{MSE}_{\text{coarse}}/\mathrm{MSE}_{\text{fine}}\right)$ across grid refinements for $\alpha = 2$, as the noise intensity σ decreases from 1 to 0.0001.

	$\Delta x = 1/50$, $\Delta t = 1/100$	$\Delta x = 1/100$, $\Delta t = 1/200$		$\Delta x = 1/200$, $\Delta t = 1/400$		$\Delta x = 1/400$, $\Delta t = 1/800$	
σ	MSE	MSE	p	MSE	p	MSE	p
1	5.787672×10^{-2}	5.338372×10^{-2}	0.058	5.253846×10^{-2}	0.012	5.246564×10^{-2}	0.001
0.1	6.475157×10^{-3}	8.926669×10^{-4}	1.429	5.383908×10^{-4}	0.365	5.348914×10^{-4}	0.005
0.01	5.976572×10^{-3}	3.802779×10^{-4}	1.987	2.869329×10^{-5}	1.864	6.815487×10^{-6}	1.037
0.001	5.972051×10^{-3}	3.750106×10^{-4}	1.997	2.359619×10^{-5}	1.996	1.530227×10^{-6}	1.974
0.0001	5.972052×10^{-3}	3.749432×10^{-4}	1.997	2.354519×10^{-5}	1.996	1.476652×10^{-6}	1.998

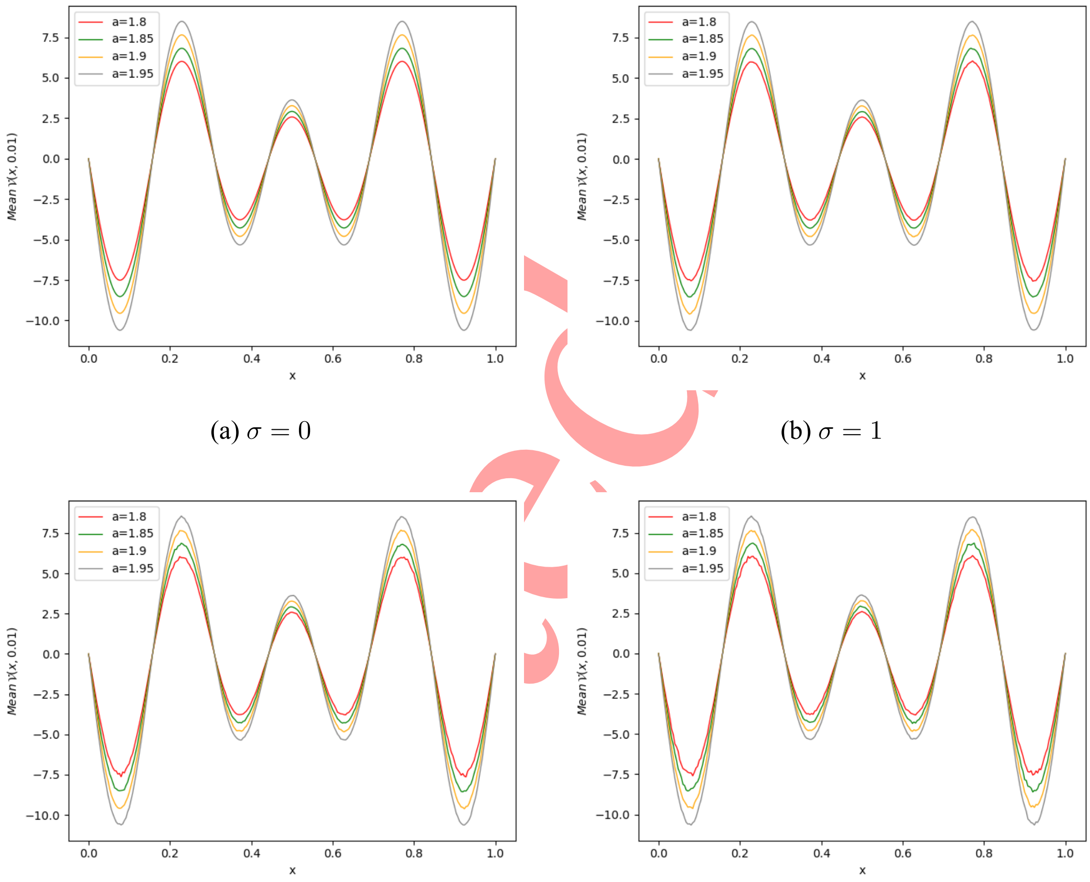

(a) $\sigma = 0$ (b) $\sigma = 1$

(c) $\sigma = 2$ (d) $\sigma = 3$

Figure 3: Approximate two-dimensional mean solutions of the TFSTWE at time $t = 0.01$ for $\alpha = 1.8, 1.85, 1.9,$ and 1.95, with $\Delta x = 1/250$ and $\Delta t = 1/500$: (a) $\sigma = 0$, (b) $\sigma = 1$, (c) $\sigma = 2$, and (d) $\sigma = 3$.

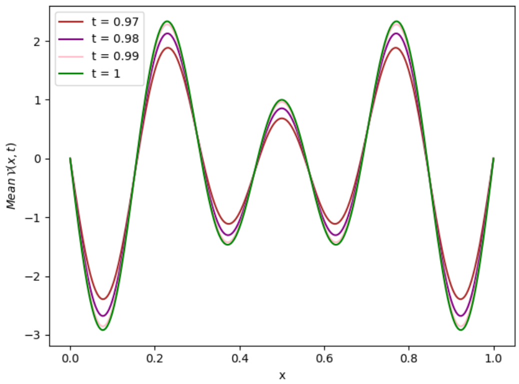

(a) $\sigma = 0$

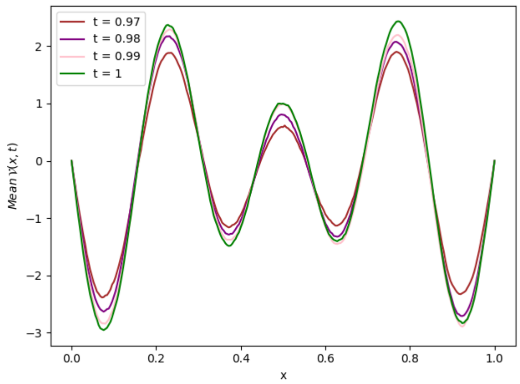

(b) $\sigma = 1$

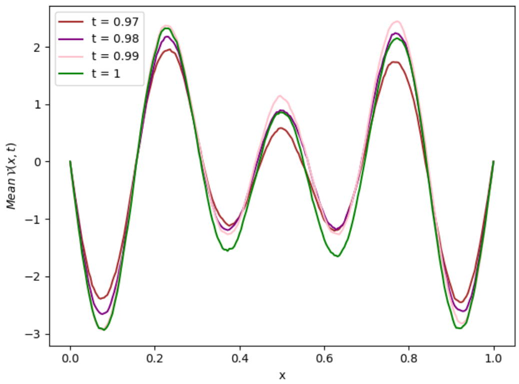

(c) $\sigma = 2$

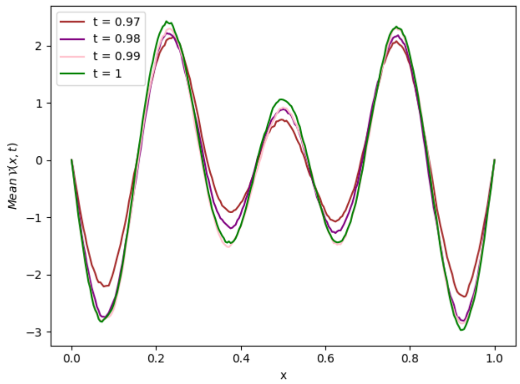

(d) $\sigma = 3$

Figure 4: Approximate two-dimensional mean solutions of the TFSTWE for $\alpha = 2$ at times $t = 0.97, 0.98, 0.99,$ and 1, with $\Delta x = 1/250$ and $\Delta t = 1/500$: (a) $\sigma = 0$, (b) $\sigma = 1$, (c) $\sigma = 2$, and (d) $\sigma = 3$.

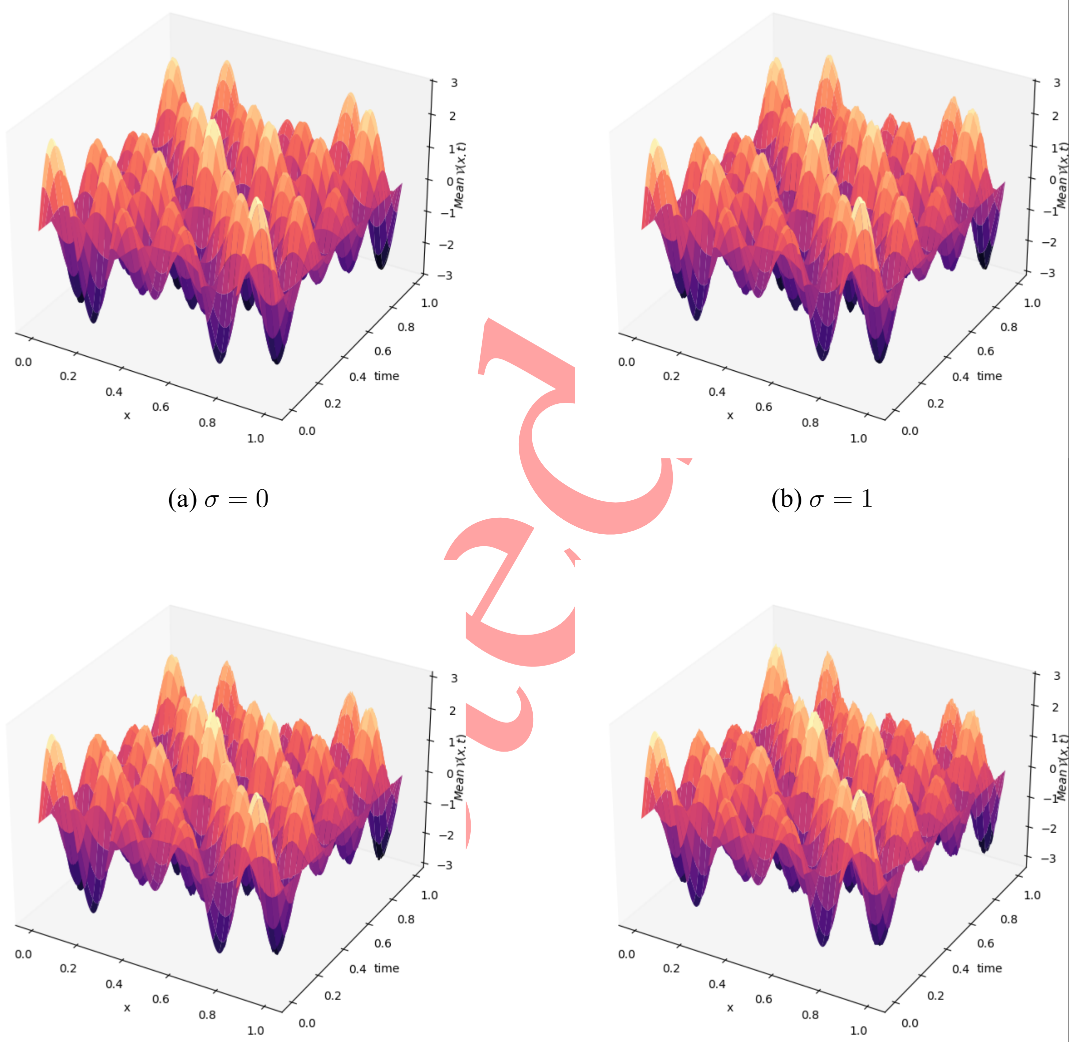

(a) $\sigma = 0$ (b) $\sigma = 1$

(c) $\sigma = 2$ (d) $\sigma = 3$

Figure 5: Approximate three-dimensional mean solutions of the TFSTWE for $\alpha = 2$, with $\Delta x = 1/250$ and $\Delta t = 1/500$: (a) $\sigma = 0$, (b) $\sigma = 1$, (c) $\sigma = 2$, and (d) $\sigma = 3$.

7 Results and Discussion

We validate the proposed scheme for the TFSTWE using graphical representations, comparisons with the exact solution, and a global MSE analysis. When the noise intensity σ is large (specifically, $\sigma \geq 1$), the stochastic fluctuations become clearly visible in the approximate mean solution profiles. These findings collectively indicate how the dynamics of the solution are shaped simultaneously by the fractional order and the stochastic component.

To examine the efficiency of the method, we performed simulations for multiple values of the fractional order α and the noise intensity σ. Figure 1 shows the parameter regimes in which the numerical solution becomes unstable, which illustrates the need for a time-step restriction such as (15) of Proposition 1. This indicates that the explicit FDM solves the TFSTWE consistently under the given conditions. Figure 2 compares the exact solution (23) with the approximate numerical solution for $\alpha = 2$ and $\sigma = 0$, which validates the accuracy of the method.

Figures 3 and 4 further examine how the stochastic term influences the two-dimensional approximate mean solutions. Figure 3 illustrates these effects for the fractional orders $\alpha \in \{1.80, 1.85, 1.90, 1.95\}$ at the early time $t = 0.01$ and for the noise intensities $\sigma \in \{0, 1, 2, 3\}$. Figure 4 shows the solutions for $\alpha = 2$ at the final times $t = 0.97$ to $t = 1$, indicating that the noise continues to influence the system as it evolves. Finally, Figure 5 presents the three-dimensional approximate mean solutions, visualizing the computed values of $\mathcal{V}(x, t)$ for $\alpha = 2$ across varying noise intensities.

Table 1 reports the global MSE and the empirical order p for $\alpha = 2$, comparing the TFSTWE with its classical limit as σ decreases from 1 to 0.0001. For $\sigma = 0.001$ and $\sigma = 0.0001$, $p \approx 2$ at all resolutions, confirming that the TFSTWE recovers the second-order accuracy of the classical scheme as $\sigma \to 0$. As σ increases, p drops below 2, and it does so earlier: for $\sigma = 0.01$, it stays near 2 until the finest grid, whereas for $\sigma = 0.1$ and $\sigma = 1$, it falls almost immediately. This occurs because the noise adds a fixed error that does not decrease with grid refinement; once this fixed error exceeds the decreasing truncation error, further refinement no longer improves the accuracy. The MSE values reflect this pattern: on the coarsest grid, the MSE is nearly identical across all small values of σ, but on the finest grid, it varies sharply with σ. This indicates that σ determines how much refinement can help, even though the scheme itself shows second-order convergence numerically for $\alpha = 2$.

8 Conclusion

In this paper, an explicit FDM was developed to solve the TFSTWE with fractional order $\alpha \in (1, 2]$. The method incorporates multiplicative space-time white noise to simulate stochastic perturbations, and the Caputo fractional derivative accounts for memory effects. The mean approximate solutions for a particular example were plotted using Python. Increasing the noise intensity makes the wave propagation increasingly irregular and stochastically perturbed, which has a major effect on the amplitude and smoothness of the solution. For the first time step, a mean-square stability bound (Proposition 1) and an error estimate (Proposition 2) were derived; stability and convergence over all time levels are supported by the numerical experiments (Table 1) and remain to be proved (Remarks 1 and 3).

Limitations. (a) A stability and convergence proof over all time levels is not provided, because the scheme contains negative weights at later time levels, so the analysis is limited to the first step and is complemented by numerical evidence; (b) the method is restricted to one spatial dimension; (c) the error analysis does not provide strong convergence rates in the probabilistic sense (only mean-square convergence of the scheme is established); and (d) no comparison with an implicit or Crank–Nicolson analogue is provided.

Future work. (1) Extension of the explicit FDM to two-dimensional domains for the TFSTWE, where the noise approximation becomes more involved and the computational cost increases substantially; (2) development of an unconditionally stable implicit or semi-implicit scheme for the multiplicative-noise TFSTWE, building on the Crank–Nicolson approach of Mojad et al. [15] to overcome the conditional stability restriction; (3) investigation of the strong convergence rate (in the $L^2(\Omega)$ sense), rather than only the mean-square convergence of the numerical scheme, using Malliavin calculus or stochastic Gronwall arguments; and (4) application of the proposed methodology to nonlinear TFSTWEs, where multiplicative noise interacts with nonlinear wave terms arising in continuum mechanics and geophysical wave modeling.

Overall, this work offers a computationally simple framework for simulating stochastic fractional wave propagation, while identifying gaps in dimensionality, the full-time stability and convergence theory, and the stability class that future work should address.

Declarations

Availability of Supporting Data

The data that support the findings of this study are available from the corresponding author upon reasonable request.

Funding

The first author gratefully acknowledges the financial support provided by the Chhatrapati Shahu Maharaj Research, Training and Human Development Institute (SARTHI), Government of Maharashtra, for funding this research work.

Conflict of Interest

The authors declare that they have no known competing financial interests or personal relationships that could have influenced the work reported in this paper.

Author Contributions

Priti Mojad: Conceptualization; Formal Analysis; Writing – Original Draft; Writing – Review & Editing; Project Administration. **Babasaheb Gavhane**: Conceptualization; Data Curation; Writing – Review & Editing; Visualization. **Shrikisan Gaikwad**: Software and Validation; Resources; Writing – Review & Editing. **Kalyanrao Takale**: Methodology; Writing – Review & Editing; Visualization. **Chetan Shirore**: Investigation; Writing – Review & Editing; Supervision.

Artificial Intelligence Statement

Artificial intelligence (AI) tools, including large language models, were used solely for language editing and improving the readability of the manuscript. AI tools were not used to generate research ideas, perform analyses, interpret results, or produce the scientific content of the study. All scientific conclusions and intellectual contributions were made exclusively by the authors.

Publisher's Note

The publisher remains neutral regarding jurisdictional claims in published maps and institutional affiliations.

References

[1] Bayer, C., Qiu, J., Yao, Y. (2022). "Pricing options under rough volatility with backward SPDEs". *SIAM Journal on Financial Mathematics*, 13, 179–212. https://doi.org/10.1137/20M1357639

[2] Chen, L., Hu, G., Hu, Y., Hu, J. (2017). "Space-time fractional diffusions in Gaussian noisy environment". *Stochastics*, 89, 171–206. https://doi.org/10.1080/17442508.2016.1146282

[3] Chukwuyem, N. J., Nkonyeasua, N. I., Apanapudor, J. S. (2025). "Crank-Nicolson finite element method for the time fractional stochastic wave equation". *Mathematics and Statistics*, 13(3), 154–162. https://doi.org/10.13189/ms.2025.130304

[4] Darehmiraki, M. (2018). "An efficient solution for stochastic fractional partial differential equations with additive noise by a meshless method". *International Journal of Applied and Computational Mathematics*, 4, 1–13. https://doi.org/10.1007/s40819-017-0455-9

[5] Demir, I. (2025). "Refinements of the Jensen inequality and estimates of the Jensen gap based on interval-valued functions". *Mathematical Methods in the Applied Sciences*, 48, 12567–12576. https://doi.org/10.1002/mma.11046

[6] Ghode, K., Takale, K., Gaikwad, S. (2021). "New technique for solving time fractional wave equation: Python". *Journal of Mathematical and Computational Science*, 11, 5327–5343. https://www.scik.org/index.php/jmcs/article/view/6048

[7] Goufo, F. D., Nieto, J. J. (2018). "Attractors for fractional differential problems of transition to turbulent flows". *Journal of Computational and Applied Mathematics*, 339, 329–342. https://doi.org/10.1016/j.cam.2017.08.026

[8] Hoult, J., Yan, Y. (2024). "Numerical approximation for a stochastic fractional differential equation driven by integrated multiplicative noise". *Mathematics*, 12(3), Art. no. 365. https://doi.org/10.3390/math12030365

[9] Kilbas, A. A., Srivastava, H. M., Trujillo, J. J. (2006). *Theory and applications of fractional differential equations*. North-Holland Mathematics Studies, 204. Amsterdam: Elsevier.

[10] Li, J., Zhang, J., Jiang, Y. (2025). "A finite difference method for Caputo generalized time fractional diffusion equations". *Fractal and Fractional*, 10, Art. no. 19. https://doi.org/10.3390/fractalfract10010019

[11] Ma, J., Ogunsolu, M., Qiu, J., Sezer, D. (2023). "Credit risk pricing in a consumption-based equilibrium framework with incomplete accounting information". *Mathematical Finance*, 33, 666–708. https://doi.org/10.1111/mafi.12386

[12] Mirzaee, F., Samadyar, N. (2020). "Combination of finite difference method and meshless method based on radial basis functions to solve fractional stochastic advection–diffusion equations". *Engineering with Computers*, 36, 1673–1686. https://doi.org/10.1007/s00366-019-00789-y

[13] Mirzaee, F., Sayevand, K., Rezaei, S., Samadyar, N. (2021). "Finite difference and spline approximation for solving fractional stochastic advection-diffusion equation". *Iranian Journal of Science and Technology, Transactions A: Science*, 45, 607–617. https://doi.org/10.1007/s40995-020-01036-6

[14] Moghaddam, B. P., Babaei, A., Dabiri, A., Galhano, A. (2024). "Fractional stochastic partial differential equations: Numerical advances and practical applications—A state of the art review". *Symmetry*, 16, Art. no. 563. https://doi.org/10.3390/sym16050563

[15] Mojad, P., Gavhane, B., Gaikwad, S., Takale, K. (2025). "Crank-Nicolson approximation to space-time fractional stochastic traveling wave equation with additive white noise". *Boletim da Sociedade Paranaense de Matemática*, 43, 1–15. https://doi.org/10.5269/bspm.77257

[16] Roth, C. H. (2002). "Difference methods for stochastic partial differential equations". *ZAMM Journal of Applied Mathematics and Mechanics*, 82, 821–830. https://doi.org/10.1002/1521-4001(200211)82:11/12<821::AID-ZAMM821>3.0.CO;2-L

[17] Sababheh, M., Choi, D. (2016). "A complete refinement of Young's inequality". *Journal of Mathematical Analysis and Applications*, 440(1), 379–393. https://doi.org/10.1016/j.jmaa.2016.03.049

[18] Singh, A. K., Mehra, M. (2023). "Difference methods for stochastic space fractional diffusion equation driven by additive space–time white noise via Wong–Zakai approximation". *Journal of Mathematical Chemistry*, 61, 47–74. https://doi.org/10.1007/s10910-022-01408-w

[19] Singh, S., Singh, S., Aggarwal, A. (2023). "A new spline technique for the time fractional diffusion-wave equation". *MethodsX*, 10, Art. no. 102007. https://doi.org/10.1016/j.mex.2023.102007

[20] Song, E. (2023). "Impact of noise on the instability of spiral waves in stochastic 2D mathematical models of human atrial fibrillation". *Journal of Biological Physics*, 49, 521–533. https://doi.org/10.1007/s10867-023-09644-0

[21] Song, J., Song, X., Xu, F. (2020). "Fractional stochastic wave equation driven by Gaussian noise rough in space". *Bernoulli*, 26(4), 2699–2726. https://doi.org/10.3150/20-BEJ1204

[22] Sun, Z., Wu, X. (2006). "A fully discrete difference scheme for a diffusion-wave system". *Applied Numerical Mathematics*, 56(2), 193–209. https://doi.org/10.1016/j.apnum.2005.03.003

[23] Week, B., Nuismer, S. L., Harmon, L. J., Krone, S. M. (2021). "A white noise approach to evolutionary ecology". *Journal of Theoretical Biology*, 521, Art. no. 110660. https://doi.org/10.1016/j.jtbi.2021.110660

[24] Zhang, Z., Karniadakis, G. E. (2017). "Numerical methods for stochastic partial differential equations with white noise". *Applied Mathematical Sciences*, 196. https://doi.org/10.1007/978-3-319-57511-7

Authors' Bio-sketches

Priti Mojad is affiliated with the Department of Mathematics, New Arts Commerce and Science College, Ahmednagar, India (affiliated to Savitribai Phule Pune University, Pune). Her research interests include fractional stochastic differential equations, numerical methods, and finite difference schemes.

Babasaheb Gavhane is affiliated with the Department of Mathematics, K. J. Somaiya College of Arts, Commerce and Science, Kopargaon, India. His research interests include fractional stochastic differential equations, fractional differential equations, numerical methods.

Shrikisan Gaikwad is affiliated with the Department of Mathematics, New Arts Commerce and Science College, Ahmednagar, India. His research interests include fractional differential equations, numerical methods, and Python-based scientific computing.

Kalyanrao Takale is affiliated with the Department of Computer Science, Jaykranti College of Computer Science and Management, Pune, India. His research interests include fractional differential equations, the Adomian decomposition method, and fractional stochastic differential equations.

Chetan Shirore is affiliated with the Department of Mathematics, K.R.T. Arts, B.H. Commerce and A.M. Science College, Nashik, India. His research interests include numerical methods for fractional stochastic equations and computational tools for mathematical typesetting. Corresponding author. Email: chetanshirore@kthmcollege.ac.in.

Received: xxx **Accepted:** xxx **Published:** xxx.
DOI: 10.30473/coam.2026.77231.1394 DOI. xxxxxxx
Volume xxx, Issue xxx, p.p. 25-23: xxx
Research Article

Open Access

Control and Optimization in Applied Mathematics - COAM

An Explicit Finite Difference Scheme for Time-Fractional Stochastic Traveling Wave Equations Driven by Multiplicative White Noise

Priti Mojad[1], Babasaheb Gavhane[2], Shrikisan Gaikwad[3], Kalyanrao Takale[4], Chetan Shirore[5] ✉

[1]Department of Mathematics, New Arts Commerce and Science College, Ahmednagar, affiliated to Savitribai Phule Pune University, Pune, India
[2]Department of Mathematics, K. J. Somaiya College of Arts, Commerce and Science, Kopargaon, India
[3]Department of Mathematics, New Arts Commerce and Science College, Ahmednagar, India
[4]Department of Computer Science, Jaykranti College of Computer Science and Management, Pune, India
[5]Department of Mathematics, K.R.T. Arts, B.H. Commerce and A.M. Science College, Nashik, India

✉ **Correspondence:**
Chetan Shirore
E-mail:
chetanshirore@kthmcollege.ac.in

How to Cite
Mojad, P., Gavhane, B., Gaikwad, S., Takale, K., Shirore, C. (2027). "An explicit finite difference scheme for time-fractional stochastic traveling wave equations driven by multiplicative white noise". *Control and Optimization in Applied Mathematics*, X(x), 25–23.
https://doi.org/10.30473/coam.2026.77231.1394

Abstract. This work addresses the numerical approximation of the time-fractional stochastic traveling wave equation (TFSTWE) with a Caputo fractional derivative of order $\alpha \in (1, 2]$ driven by multiplicative space-time white noise. An explicit finite difference method (FDM) is constructed by discretizing the space domain. For the first time step, a mean-square stability bound and an error estimate of order $\mathcal{O}(\Delta t^{2-\alpha} + \Delta x^2)$ are derived under a restriction on Δt that depends explicitly on Δx, the diffusion coefficient $\mathcal{K}$, and the fractional order α, while the noise intensity σ enters the mean-square growth constant; stability and convergence at later time levels are supported numerically. Comprehensive numerical experiments demonstrate the effectiveness and reliability of the proposed method, and the Python programming language is used to plot the approximate mean solution profiles in two and three dimensions. The outcomes confirm the suitability of the method for accurately solving TFSTWEs under stochastic perturbations and support the theoretical analysis.

Keywords. Explicit difference approximation, Fractional derivatives, Mean square method, Multiplicative white noise.

MSC. 60H15; 26A33; 65M06.

1 Introduction

Fractional stochastic calculus offers a natural framework for capturing randomness and memory effects in complex systems. Combining fractional calculus with stochastic processes such as Brownian motion and white noise makes it possible to describe accurately systems that exhibit long-term dependence and uncertainty [4]. Fractional stochastic differential equations (FSDEs) incorporate both memory and uncertainty effects, and they work well precisely where classical differential equations fall short in capturing uncertainty and long memory. When white noise is present, FSDEs are generally interpreted in infinite-dimensional probability spaces and are often formulated using Caputo derivatives [2]. These equations have found applications in several fields: in biology, to describe disease propagation and population dynamics under stochastic impacts [20, 23]; in finance, to capture long-memory features of market dynamics [1, 11]; and in physics, to model turbulence and thermal memory effects [7, 21].

To solve FSDEs, a variety of numerical techniques have been developed, such as Adomian decomposition, spectral methods, finite element methods, and finite difference methods [12, 14]. Finite difference schemes stand out for their simplicity, flexibility, and ease of implementation on structured grids. Explicit finite difference method (FDM) schemes are computationally simple and easy to implement, although they come with a conditional stability requirement. They also suit real-world FSDE applications well, since they can be readily adapted to higher-dimensional problems and to random disturbances [24]. Moghaddam et al. [14] reviewed in detail the development of FDM, spectral, and meshless approaches for fractional stochastic partial differential equations, including both additive and multiplicative white noise cases.

Other researchers have proposed various discretization approaches for FSDEs. Singh et al. [19] introduced a cubic B-spline-based collocation technique that solves the fractional diffusion-wave equation with higher precision and lower computational cost. Chukwuyem et al. [3] addressed time-fractional stochastic wave equations using the Crank–Nicolson finite element method (CNFEM), which offers a stable and reliable numerical framework. By combining finite difference schemes with Python-based visualizations, Ghode et al. [6] developed a computational framework for solving time-fractional wave equations. Singh and Mehra [18] proposed difference schemes for stochastic space-fractional diffusion equations with additive space–time white noise using the Wong–Zakai approximation and a shifted Grünwald–Letnikov formula. Hoult and Yan [8] proposed a numerical scheme for Caputo-type stochastic fractional differential equations with integrated multiplicative noise, approximating the noise by a piecewise constant function. Li et al. [10] developed a finite difference method for Caputo generalized time-fractional diffusion equations, extending the L1 scheme in time and using central differences in space. Mojad et al. [15] employed a Crank–Nicolson finite difference scheme for space–time fractional stochastic traveling wave equations with additive white noise, where the noise is independent of the solution. Unlike this additive case, multiplicative noise couples directly with the solution, which introduces additional challenges and motivates the present work.

In the present work, we employ an explicit FDM to solve the TFSTWE driven by multiplicative space-time white noise. The TFSTWE considered here, together with its initial and boundary conditions, is given by

$$
\begin{aligned}
{}^{C}\mathscr{D}_t^{\alpha}\mathcal{V}(x,t) &= \mathcal{K}^2\,\frac{\partial^2\mathcal{V}(x,t)}{\partial x^2} + \sigma\,\mathcal{V}(x,t)\,\dot{\mathcal{W}}(x,t), \\
&\qquad\qquad 0 < x \le \mathcal{L},\ 0 < t \le \mathcal{T},\ 1 < \alpha \le 2, && \text{(1a)}\\
\mathcal{V}(x,0) &= \Psi_1(x), && \text{(1b)}\\
\mathcal{V}_t(x,0) &= \Psi_2(x), && \text{(1c)}\\
\mathcal{V}(0,t) &= 0, && \text{(1d)}\\
\mathcal{V}(\mathcal{L},t) &= 0. && \text{(1e)}
\end{aligned}
$$

The term ${}^{C}\mathscr{D}_t^{\alpha}\mathcal{V}(x,t)$ denotes the Caputo fractional derivative of order $\alpha \in (1,2]$ of the stochastic process $\mathcal{V}(x,t)$. The functions $\Psi_1(x)$ and $\Psi_2(x)$ are known initial data, assumed to be bounded and continuous on $[0,\mathcal{L}]$, which ensures the existence of a unique solution to the model (1). Here, σ denotes the noise amplitude, and $\mathcal{L}$, $\mathcal{K}$, and $\mathcal{T}$ are positive constants. The term $\dot{\mathcal{W}}(x,t)$ is a space-time white noise defined on a filtered probability space $(\Omega,\mathcal{F},\{\mathcal{F}_t\}_{t\ge 0},\mathbb{P})$, where Ω is the sample space of all possible outcomes, $\mathcal{F}$ is the complete σ-algebra of events, and the filtration $\{\mathcal{F}_t\}_{t\ge 0}$ satisfies the usual conditions of right-continuity and completeness. Throughout this paper, $\dot{\mathcal{W}}(x,t)$ is a generalized Gaussian process with zero mean and the delta-correlated covariance structure

$$
\mathbb{E}\big[\dot{\mathcal{W}}(x,t)\,\dot{\mathcal{W}}(s,y)\big] = \delta(x-s)\,\delta(t-y),
$$

where $\delta(\cdot)$ denotes the Dirac delta function. This is the distributional derivative of the Brownian sheet and corresponds to space-time white noise.

The remainder of this paper is organized as follows. Section 2 introduces the essential definitions and lemmas from fractional stochastic calculus. Section 3 describes the proposed numerical scheme in detail. The mean-square stability and the error of the first time step are analyzed in Sections 4 and 5, respectively, together with a discussion of the difficulties at later time levels. Section 6 presents a numerical example implemented in Python, in which the behavior of the solution is illustrated graphically to show how the dynamics of the system are affected by both random perturbations and the fractional order. The results are discussed in Section 7, and Section 8 concludes the paper.

2 Preliminaries

This section reviews the essential definitions and lemmas from fractional stochastic calculus that are used in the subsequent analysis.

Definition 1. Let w be a continuous real-valued function defined on $[0,\infty)$. For a fractional order $\alpha > 0$ such that $n-1 < \alpha \leq n$ with $n \in \mathbb{N}$, the Caputo fractional derivative [9] is defined by

$$\mathcal{D}_t^{\alpha} w(t) := \begin{cases} \dfrac{1}{\Gamma(n-\alpha)} \displaystyle\int_0^t (t-\zeta)^{n-\alpha-1}\, w^{(n)}(\zeta)\, d\zeta, & \text{if } n-1 < \alpha < n, \\ w^{(n)}(t), & \text{if } \alpha = n \in \mathbb{N}, \end{cases}$$

where $w^{(n)}$ denotes the classical derivative of order n of w. The Euler gamma function $\Gamma(\cdot)$ is defined for $p > 0$ by

$$\Gamma(p) := \int_0^\infty e^{-x} x^{p-1}\, dx.$$

Definition 2. A stochastic difference scheme is said to be stable in the mean-square sense [16] if there exist positive constants ϵ and δ and non-negative constants λ and v such that

$$\mathbb{E}\left\|\mathcal{U}^{n+1}\right\|_\infty^2 \leq \lambda\, e^{vt}\, \mathbb{E}\left\|\mathcal{U}^0\right\|_\infty^2$$

for all $t = (n+1)\Delta t$, where $\mathbb{E}[\cdot]$ is the mathematical expectation operator on the probability space $(\Omega, \mathcal{F}, \mathbb{P})$. The time step Δt and the space step Δx must satisfy $0 < \Delta x \leq \epsilon$ and $0 < \Delta t \leq \delta$. A difference scheme is called unconditionally stable if no restriction is imposed on the relation between Δx and Δt; otherwise, it is called conditionally stable.

Definition 3. A stochastic difference scheme $\mathcal{L}_i^m \mathcal{S}_i^m = \mathcal{G}_i^m$ that approximates a stochastic differential equation (SDE) $\mathcal{L}\mathcal{S} = \mathcal{G}$ at time $t = (m+1)\Delta t$ is said to be convergent in the mean-square sense [13] if

$$\mathbb{E}\left\|\mathcal{S}_i^m - \mathcal{S}\right\|_\infty^2 \to 0 \quad \text{as } i\Delta x \to x,\ m\Delta t \to t,\ \Delta x \to 0,\ \Delta t \to 0.$$

Lemma 1 (Sun and Wu [22])**.** Let $b_j = (j+1)^{2-\alpha} - j^{2-\alpha}$ for $j = 1, 2, \dots$ and $\alpha > 0$. Then

1. $b_j > 0$ (positivity);
2. $b_j > b_{j+1}$ (monotonically decreasing);
3. $b_{j+1} - b_j < b_j - b_{j-1}$ (convexity).

Lemma 2 (Young's inequality)**.** For real numbers x, y and any $\epsilon > 0$,

$$(x+y)^2 \leq (1+\epsilon)x^2 + \left(1 + \frac{1}{\epsilon}\right)y^2.$$

Proof. By Young's inequality [17], $x^{\nu}y^{1-\nu} \leq \nu x + (1-\nu)y$ for $x, y > 0$ and $0 \leq \nu \leq 1$. Setting $\nu = \frac{1}{2}$ gives $\sqrt{xy} \leq \frac{x+y}{2}$. Substituting $x \to \epsilon x^2$ and $y \to y^2/\epsilon$ yields $|xy| \leq \frac{\epsilon}{2}x^2 + \frac{1}{2\epsilon}y^2$. Hence

$$(x+y)^2 = x^2 + 2xy + y^2 \leq x^2 + 2|xy| + y^2 \leq (1+\epsilon)x^2 + \left(1 + \frac{1}{\epsilon}\right)y^2. \qquad \square$$

Lemma 3 (Jensen's inequality)**.** Let $w_1, w_2, \ldots, w_m \geq 0$ be weights satisfying $\sum_{j=1}^{m} w_j = 1$, and let $x_1, x_2, \ldots, x_m$ be real numbers. Then

$$\left(\sum_{j=1}^{m} w_j\, x_j\right)^2 \leq \sum_{j=1}^{m} w_j\, x_j^2.$$

Proof. By Jensen's inequality [5], for any convex function f,

$$f\left(\sum_{j=1}^{m} w_j\, x_j\right) \leq \sum_{j=1}^{m} w_j\, f(x_j).$$

Since $f(x) = x^2$ is convex, the result follows immediately. $\square$

3 Numerical Scheme

This section presents the explicit difference approximation used to solve the TFSTWE. To develop the numerical scheme for the proposed model (1), we use the following notation. Let $\mathcal{C} = \{t_n = n\Delta t \mid \Delta t = \mathcal{T}/\mathcal{M},\ n = 0, 1, 2, \ldots, \mathcal{M}\}$ be a set of uniformly distributed points in the interval $[0, \mathcal{T}]$. Likewise, let $\mathcal{D} = \{x_i = i\Delta x \mid \Delta x = \mathcal{L}/\mathcal{N},\ i = 0, 1, 2, \ldots, \mathcal{N}\}$ be a set of uniformly distributed points in the interval $[0, \mathcal{L}]$. The quantity $\mathcal{V}_i^n$ denotes the numerical approximation of the exact solution $\mathcal{V}(x_i, t_n)$ at the mesh point (x_i, t_n).

3.1 Approximation in Time

According to Definition 1, ${}^{C}\mathscr{D}_t^{\alpha}\mathcal{V}(x,t)$ can be written as

$${}^{C}\mathscr{D}_t^{\alpha}\mathcal{V}(x,t) = \begin{cases} \dfrac{1}{\Gamma(2-\alpha)} \displaystyle\int_0^t (t-s)^{1-\alpha}\, \frac{\partial^2 \mathcal{V}(x,s)}{\partial s^2}\, ds, & 1 < \alpha < 2,\ x > 0, \\[2ex] \dfrac{\partial^2 \mathcal{V}(x,t)}{\partial t^2}, & \alpha = 2. \end{cases}$$

At the mesh points (x_i, t_n), $i = 1, 2, \ldots, \mathcal{N}-1$ and $n = 1, 2, \ldots, \mathcal{M}-1$, the time-fractional derivative for $1 < \alpha < 2$ is

$$ {}^{C}\mathscr{D}_t^{\alpha}\mathcal{V}(x_i,t_n) = \frac{1}{\Gamma(2-\alpha)}\int_0^{t_n}(t_n-s)^{1-\alpha}\,\frac{\partial^2\mathcal{V}(x_i,s)}{\partial s^2}\,ds. $$

Using the substitution property $\int_0^a f(x)\,dx = \int_0^a f(a-x)\,dx$, which holds for any continuous function f defined on $[0,a]$, and splitting the integration interval into the subintervals $[t_j,t_{j+1}]$, we obtain

$$ \begin{aligned} {}^{C}\mathscr{D}_t^{\alpha}\mathcal{V}(x_i,t_n) &= \frac{1}{\Gamma(2-\alpha)}\int_0^{t_n} s^{1-\alpha}\,\frac{\partial^2\mathcal{V}(x_i,t_n-s)}{\partial s^2}\,ds \\ &= \frac{1}{\Gamma(2-\alpha)}\sum_{j=0}^{n-1}\int_{t_j}^{t_{j+1}} s^{1-\alpha}\,\frac{\partial^2\mathcal{V}(x_i,t_n-s)}{\partial s^2}\,ds \\ &= \frac{1}{\Gamma(2-\alpha)}\sum_{j=0}^{n-1}\int_{t_j}^{t_{j+1}} s^{1-\alpha} \\ &\qquad\times\Big(\frac{\mathcal{V}(x_i,t_n-t_{j+1})+\mathcal{V}(x_i,t_n-t_{j-1})-2\mathcal{V}(x_i,t_n-t_j)}{\Delta t^2} \\ &\qquad\quad + \mathcal{O}(\Delta t^{2-\alpha})\Big)ds \\ &= \frac{1}{\Gamma(2-\alpha)}\sum_{j=0}^{n-1}\Big(\frac{\mathcal{V}(x_i,t_n-t_{j-1})+\mathcal{V}(x_i,t_n-t_{j+1})-2\mathcal{V}(x_i,t_n-t_j)}{\Delta t^2} \\ &\qquad + \mathcal{O}(\Delta t^{2-\alpha})\Big) \\ &\qquad\times\Big(\frac{s^{2-\alpha}}{2-\alpha}\Big)_{t_j}^{t_{j+1}} \\ &= \frac{1}{\Gamma(2-\alpha)}\sum_{j=0}^{n-1}\Big(\frac{\mathcal{V}_i^{n+1-j}+\mathcal{V}_i^{n-1-j}-2\mathcal{V}_i^{n-j}}{\Delta t^2} \\ &\qquad + \mathcal{O}(\Delta t^{2-\alpha})\Big) \\ &\qquad\times\Big(\frac{t_{j+1}^{2-\alpha}-t_j^{2-\alpha}}{2-\alpha}\Big) \\ &= \frac{1}{\Gamma(2-\alpha)}\sum_{j=0}^{n-1}\Big(\frac{\mathcal{V}_i^{n+1-j}+\mathcal{V}_i^{n-1-j}-2\mathcal{V}_i^{n-j}}{\Delta t^2} \\ &\qquad + \mathcal{O}(\Delta t^{2-\alpha})\Big) \\ &\qquad\times\Big(\frac{((j+1)\Delta t)^{2-\alpha}-(j\Delta t)^{2-\alpha}}{2-\alpha}\Big) \\ &= \frac{(\Delta t)^{2-\alpha}}{(2-\alpha)\,\Gamma(2-\alpha)}\sum_{j=0}^{n-1}\Big(\frac{\mathcal{V}_i^{n+1-j}+\mathcal{V}_i^{n-1-j}-2\mathcal{V}_i^{n-j}}{\Delta t^2} \\ &\qquad + \mathcal{O}(\Delta t^{2-\alpha})\Big) \\ &\qquad\times\big((j+1)^{2-\alpha}-j^{2-\alpha}\big) \end{aligned} $$

$$
\begin{aligned}
&= \frac{(\Delta t)^{-\alpha}}{\Gamma(3-\alpha)} \sum_{j=0}^{n-1} \big(\mathcal{V}_i^{n+1-j} + \mathcal{V}_i^{n-1-j} - 2\mathcal{V}_i^{n-j}\big)\big((j+1)^{2-\alpha} - j^{2-\alpha}\big) \\
&\quad + \frac{(\Delta t)^{2-\alpha}\, \mathcal{O}(\Delta t^{2-\alpha})}{\Gamma(3-\alpha)} \sum_{j=0}^{n-1} \big((j+1)^{2-\alpha} - j^{2-\alpha}\big) \\
&= \frac{(\Delta t)^{-\alpha}}{\Gamma(3-\alpha)} \sum_{j=0}^{n-1} \big(\mathcal{V}_i^{n+1-j} + \mathcal{V}_i^{n-1-j} - 2\mathcal{V}_i^{n-j}\big)\big((j+1)^{2-\alpha} - j^{2-\alpha}\big) \\
&\quad + \frac{(n\Delta t)^{2-\alpha}\, \mathcal{O}(\Delta t^{2-\alpha})}{\Gamma(3-\alpha)}.
\end{aligned}
$$

Clearly, if $n\Delta t < \infty$, then $(n\Delta t)^{2-\alpha}\, \mathcal{O}(\Delta t^{2-\alpha})/\Gamma(3-\alpha) = \mathcal{O}(\Delta t^{2-\alpha})$. Therefore, the Caputo fractional derivative of order $1 < \alpha < 2$ is approximated, with an error of order $\mathcal{O}(\Delta t^{2-\alpha})$, by

$$
{}^{C}\mathscr{D}_t^{\alpha}\mathcal{V}(x_i, t_n) = \frac{(\Delta t)^{-\alpha}}{\Gamma(3-\alpha)} \sum_{j=0}^{n-1} b_j \big(\mathcal{V}_i^{n+1-j} + \mathcal{V}_i^{n-1-j} - 2\mathcal{V}_i^{n-j}\big), \tag{2}
$$

where $b_j = (j+1)^{2-\alpha} - j^{2-\alpha}$.

3.2 Approximation in Space

At the mesh points (x_i, t_n), $i = 1, 2, \ldots, \mathcal{N} - 1$ and $n = 1, 2, \ldots, \mathcal{M} - 1$, the second-order space derivative is approximated by the central difference

$$
\frac{\partial^2 \mathcal{V}(x_i, t_n)}{\partial x^2} = \frac{\mathcal{V}_{i+1}^n + \mathcal{V}_{i-1}^n - 2\mathcal{V}_i^n}{(\Delta x)^2} + \mathcal{O}\big((\Delta x)^2\big). \tag{3}
$$

3.3 Approximation of the Noise Term

To simulate the stochastic system numerically, we employ the Brownian sheet $\mathcal{W}(x, t)$ over the domain $[0, \mathcal{L}] \times [0, \mathcal{T}]$. Following Hoult and Yan [8], a two-dimensional Brownian sheet satisfies the following properties.

1. *Boundary values:* $\mathcal{W}(x, 0) = \mathcal{W}(0, t) = 0$ for all $x \in [0, \mathcal{L}]$ and $t \in [0, \mathcal{T}]$.
2. *Gaussian increments:* For any rectangle $\mathcal{R} = [x_i, x_{i+1}] \times [t_n, t_{n+1}]$, the rectangular increment

   $$
   \Delta\mathcal{W}(x_i, t_n) = \mathcal{W}(x_{i+1}, t_{n+1}) - \mathcal{W}(x_i, t_{n+1}) - \mathcal{W}(x_{i+1}, t_n) + \mathcal{W}(x_i, t_n),
   $$

   is normally distributed with mean zero and variance $\Delta x\, \Delta t$, that is, $\Delta\mathcal{W} \sim \mathcal{N}(0, \Delta x\, \Delta t)$.

3. *Independent increments:* Increments over disjoint rectangles are independent.

The space-time white noise $\dot{\mathcal{W}}(x,t)$ is formally related to the Brownian sheet through the mixed partial derivative $\dot{\mathcal{W}}(x,t) = \partial^2 \mathcal{W}(x,t)/\partial x\,\partial t$. On a regular grid with time step Δt and space step Δx, the noise term at each grid point (x_i, t_n) is approximated as

$$\begin{aligned}\dot{\mathcal{W}}(x_i,t_n) &\approx \frac{\Delta \mathcal{W}}{\Delta x\,\Delta t} \approx \frac{\mathcal{N}(0,\Delta x\,\Delta t)}{\Delta x\,\Delta t}\\ &\approx \frac{\sqrt{\Delta x\,\Delta t}\,\mathcal{N}(0,1)}{\Delta x\,\Delta t} \approx \frac{\mathcal{X}_i^n}{\sqrt{\Delta x\,\Delta t}},\end{aligned} \tag{4}$$

where $\mathcal{X}_i^n \sim \mathcal{N}(0,1)$ are independent and identically distributed (i.i.d.) Gaussian random variables with zero mean and unit variance.

3.4 Scheme Formulation for the Given Model

Combining the approximations (2), (3), and (4) derived in Sections 3.1–3.3, the numerical approximation of the TFSTWE (1a) takes the form

$$\begin{aligned}&\frac{(\Delta t)^{-\alpha}}{\Gamma(3-\alpha)}\sum_{j=0}^{n-1} b_j\big(\mathcal{V}_i^{n+1-j} + \mathcal{V}_i^{n-1-j} - 2\mathcal{V}_i^{n-j}\big)\\ &\qquad = \mathcal{K}^2\,\frac{\mathcal{V}_{i+1}^n + \mathcal{V}_{i-1}^n - 2\mathcal{V}_i^n}{(\Delta x)^2} + \sigma\,\mathcal{V}_i^n\,\frac{\mathcal{X}_i^n}{\sqrt{\Delta x\,\Delta t}},\\ &\sum_{j=0}^{n-1} b_j\big(\mathcal{V}_i^{n+1-j} + \mathcal{V}_i^{n-1-j} - 2\mathcal{V}_i^{n-j}\big)\\ &\qquad = \frac{\mathcal{K}^2\,\Gamma(3-\alpha)}{(\Delta t)^{-\alpha}}\,\frac{\mathcal{V}_{i+1}^n + \mathcal{V}_{i-1}^n - 2\mathcal{V}_i^n}{(\Delta x)^2} + \frac{\Gamma(3-\alpha)\,\sigma}{(\Delta t)^{-\alpha}}\,\mathcal{V}_i^n\,\frac{\mathcal{X}_i^n}{\sqrt{\Delta x\,\Delta t}},\\ &\sum_{j=0}^{n-1} b_j\big(\mathcal{V}_i^{n+1-j} + \mathcal{V}_i^{n-1-j} - 2\mathcal{V}_i^{n-j}\big)\\ &\qquad = \frac{\mathcal{K}^2\,\Gamma(3-\alpha)}{(\Delta t)^{-\alpha}(\Delta x)^2}\big(\mathcal{V}_{i+1}^n + \mathcal{V}_{i-1}^n - 2\mathcal{V}_i^n\big) + \frac{\sigma\,\Gamma(3-\alpha)}{(\Delta t)^{0.5-\alpha}(\Delta x)^{0.5}}\,\mathcal{V}_i^n\,\mathcal{X}_i^n,\\ &\sum_{j=0}^{n-1} b_j\big(\mathcal{V}_i^{n+1-j} + \mathcal{V}_i^{n-1-j} - 2\mathcal{V}_i^{n-j}\big)\\ &\qquad = \frac{\mathcal{K}^2\,\Gamma(3-\alpha)(\Delta t)^{\alpha}}{(\Delta x)^2}\big(\mathcal{V}_{i+1}^n + \mathcal{V}_{i-1}^n - 2\mathcal{V}_i^n\big) + \frac{\sigma\,\Gamma(3-\alpha)(\Delta t)^{\alpha-0.5}}{(\Delta x)^{0.5}}\,\mathcal{V}_i^n\,\mathcal{X}_i^n.\end{aligned}$$

Separating the term $j = 0$ (recall that $b_0 = 1$) from the sum gives

$$\begin{aligned}&\mathcal{V}_i^{n+1} + \mathcal{V}_i^{n-1} - 2\mathcal{V}_i^n + \sum_{j=1}^{n-1} b_j\big(\mathcal{V}_i^{n+1-j} + \mathcal{V}_i^{n-1-j} - 2\mathcal{V}_i^{n-j}\big)\\ &\qquad = a\big[\mathcal{V}_{i+1}^n + \mathcal{V}_{i-1}^n - 2\mathcal{V}_i^n\big] + c\,\mathcal{V}_i^n\,\mathcal{X}_i^n,\end{aligned} \tag{5}$$

where

$$a = \frac{\mathcal{K}^2\,\Gamma(3-\alpha)(\Delta t)^{\alpha}}{(\Delta x)^2}, \qquad c = \frac{\sigma\,\Gamma(3-\alpha)(\Delta t)^{\alpha-0.5}}{(\Delta x)^{0.5}},$$
$$b_j = (j+1)^{2-\alpha} - j^{2-\alpha}, \tag{6}$$

and $\mathcal{X}_i^n \sim \mathcal{N}(0,1)$.

The initial conditions (1b) and (1c) are approximated as

$$\mathcal{V}_i^0 = \Psi_1(x_i), \qquad i = 0,1,2,\ldots,\mathcal{N}, \tag{7}$$
$$\mathcal{V}_i^{-1} = \mathcal{V}_i^1 - 2\,\Delta t\,\Psi_2(x_i), \qquad i = 0,1,2,\ldots,\mathcal{N}, \tag{8}$$

and the boundary conditions (1d) and (1e) take the form

$$\mathcal{V}_0^n = 0, \qquad n = 0,1,2,\ldots,\mathcal{M}, \tag{9}$$
$$\mathcal{V}_{\mathcal{N}}^n = 0, \qquad n = 0,1,2,\ldots,\mathcal{M}. \tag{10}$$

For $n = 0$, Equation (5) reduces to

$$\begin{aligned}
\mathcal{V}_i^1 + \mathcal{V}_i^{-1} - 2\mathcal{V}_i^0 &= a\big(\mathcal{V}_{i+1}^0 + \mathcal{V}_{i-1}^0 - 2\mathcal{V}_i^0\big) + c\,\mathcal{V}_i^0\mathcal{X}_i^0,\\
\mathcal{V}_i^1 + \big(\mathcal{V}_i^1 - 2\,\Delta t\,\Psi_2(x_i)\big) - 2\mathcal{V}_i^0 &= a\big(\mathcal{V}_{i+1}^0 + \mathcal{V}_{i-1}^0 - 2\mathcal{V}_i^0\big) + c\,\mathcal{V}_i^0\mathcal{X}_i^0,\\
\mathcal{V}_i^1 &= \frac{a}{2}\,\mathcal{V}_{i-1}^0 + \frac{a}{2}\,\mathcal{V}_{i+1}^0 + (1-a)\,\mathcal{V}_i^0 + \Delta t\,\Psi_2(x_i) + \frac{c}{2}\,\mathcal{V}_i^0\mathcal{X}_i^0,
\end{aligned}$$

where (8) has been used in the second line. The complete discretization of the TFSTWE is therefore given by

$$\mathcal{V}_i^1 = \frac{a}{2}\,\mathcal{V}_{i-1}^0 + \frac{a}{2}\,\mathcal{V}_{i+1}^0 + (1-a)\,\mathcal{V}_i^0 + \Delta t\,\Psi_2(x_i) + \frac{c}{2}\,\mathcal{V}_i^0\mathcal{X}_i^0, \qquad n = 0, \tag{11}$$

and, for $n \geq 1$,

$$\begin{aligned}
\mathcal{V}_i^{n+1} &= a\,\mathcal{V}_{i-1}^n + a\,\mathcal{V}_{i+1}^n + (2-2a-b_1)\,\mathcal{V}_i^n + (2b_1-b_2-1)\,\mathcal{V}_i^{n-1}\\
&\quad - \sum_{j=2}^{n-2}(b_{j-1}+b_{j+1}-2b_j)\,\mathcal{V}_i^{n-j} + (2b_{n-1}-b_{n-2})\,\mathcal{V}_i^1 - b_{n-1}\,\mathcal{V}_i^0 + c\,\mathcal{V}_i^n\mathcal{X}_i^n.
\end{aligned} \tag{12}$$

3.5 Matrix Representation of the Derived Scheme

Let

$$\mathcal{V}^n = \begin{bmatrix} \mathcal{V}_1^n \\ \mathcal{V}_2^n \\ \vdots \\ \mathcal{V}_{\mathcal{N}-1}^n \end{bmatrix}, \qquad \mathcal{X}^n = \begin{bmatrix} \mathcal{X}_1^n \\ \mathcal{X}_2^n \\ \vdots \\ \mathcal{X}_{\mathcal{N}-1}^n \end{bmatrix},$$

$$\mathcal{H} = \begin{bmatrix} \Delta t\, \Psi_2(x_1) \\ \Delta t\, \Psi_2(x_2) \\ \vdots \\ \Delta t\, \Psi_2(x_{\mathcal{N}-1}) \end{bmatrix},$$

and let $\mathcal{I}$ denote the identity matrix of order $(\mathcal{N}-1) \times (\mathcal{N}-1)$. The product $\mathcal{V}^n \mathcal{X}^n$ below is understood componentwise. The complete discretized TFSTWE, given by (11) and (12), can then be written in matrix form as

$$\mathcal{V}^1 = \mathcal{Q}_1 \mathcal{V}^0 + \mathcal{H} + \frac{c}{2} \mathcal{V}^0 \mathcal{X}^0, \qquad n = 0, \tag{13}$$

and, for $n \geq 1$,

$$\begin{aligned} \mathcal{V}^{n+1} = \mathcal{Q}_2 \mathcal{V}^n + (2b_1 - b_2 - 1)\, \mathcal{V}^{n-1} - \sum_{j=2}^{n-2} (b_{j+1} + b_{j-1} - 2b_j)\, \mathcal{V}^{n-j} \\ + (2b_{n-1} - b_{n-2})\, \mathcal{V}^1 - b_{n-1}\, \mathcal{V}^0 + c\, \mathcal{V}^n \mathcal{X}^n, \end{aligned} \tag{14}$$

where $\mathcal{Q}_1$ and $\mathcal{Q}_2$ are matrices of order $(\mathcal{N}-1) \times (\mathcal{N}-1)$ with entries

$$\mathcal{Q}_1 = (r_{ij}), \quad r_{ij} = \begin{cases} 1 - a, & j = i, \\ a/2, & j = i - 1, \\ a/2, & j = i + 1, \\ 0, & \text{otherwise}, \end{cases}$$

$$\mathcal{Q}_2 = (s_{ij}), \quad s_{ij} = \begin{cases} 2 - 2a - b_1, & j = i, \\ a, & j = i - 1, \\ a, & j = i + 1, \\ 0, & \text{otherwise}. \end{cases}$$

4 Stability Analysis

This section analyzes the mean-square behavior of the proposed scheme. The analysis is carried out for the first time step, where all weights of the scheme are non-negative under the restriction on Δt; the difficulty at later time levels is explained in Remark 1.

Proposition 1 (One-step mean-square bound)**.** Suppose that Δx and Δt satisfy the restriction

$$\Delta t \leq \left[\frac{(\Delta x)^2 (3 - 2^{2-\alpha})}{2\, \mathcal{K}^2\, \Gamma(3 - \alpha)} \right]^{1/\alpha}. \tag{15}$$

Then the first step (11) of the explicit finite difference scheme for the TFSTWE (1) satisfies

$$\mathbb{E}\left\|\mathcal{V}^{1}\right\|_{\infty}^{2} \leq (1+\lambda\Delta t)\,\mathbb{E}\left\|\mathcal{V}^{0}\right\|_{\infty}^{2} + 2\big(\Delta t+\Delta t^{2}\big)\left\|\Psi_{2}\right\|_{\infty}^{2}, \tag{16}$$

where

$$\lambda = 1 + \frac{\sigma^{2}\Gamma(3-\alpha)^{2}(\Delta t)^{2\alpha-2}}{\Delta x} + \frac{\sigma^{2}\Gamma(3-\alpha)^{2}(\Delta t)^{2\alpha-3}}{\Delta x}, \tag{17}$$

$\mathbb{E}\left\|\mathcal{V}^{n}\right\|_{\infty}^{2} := \sup_{1\leq i\leq \mathcal{N}-1}\mathbb{E}\left|\mathcal{V}_{i}^{n}\right|^{2}$, and $\left\|\Psi_{2}\right\|_{\infty} := \sup_{1\leq i\leq\mathcal{N}-1}\left|\Psi_{2}(x_{i})\right|$.

Proof. Set $\mathcal{S}_i := \frac{a}{2}\,\mathcal{V}_{i-1}^{0} + \frac{a}{2}\,\mathcal{V}_{i+1}^{0} + (1-a)\,\mathcal{V}_{i}^{0}$. By Equation (11),

$$\mathcal{V}_{i}^{1} = \mathcal{S}_i + \frac{c}{2}\,\mathcal{V}_{i}^{0}\mathcal{X}_{i}^{0} + \Delta t\,\Psi_{2}(x_i).$$

Applying Lemma 2 with $\epsilon = \Delta t$ to the decomposition $x = \mathcal{S}_i$ and $y = \frac{c}{2}\,\mathcal{V}_{i}^{0}\mathcal{X}_{i}^{0} + \Delta t\,\Psi_{2}(x_i)$, and then the elementary inequality $(y_1+y_2)^2 \leq 2y_1^2 + 2y_2^2$, we obtain

$$\begin{aligned}
\left|\mathcal{V}_{i}^{1}\right|^{2} &\leq (1+\Delta t)\left|\mathcal{S}_i\right|^{2} + \left(1+\frac{1}{\Delta t}\right)\left|\frac{c}{2}\,\mathcal{V}_{i}^{0}\mathcal{X}_{i}^{0} + \Delta t\,\Psi_{2}(x_i)\right|^{2} \\
&\leq (1+\Delta t)\left|\mathcal{S}_i\right|^{2} + \frac{1}{2}\left(1+\frac{1}{\Delta t}\right)c^{2}\left|\mathcal{V}_{i}^{0}\mathcal{X}_{i}^{0}\right|^{2} \\
&\quad + 2\left(1+\frac{1}{\Delta t}\right)(\Delta t)^{2}\left|\Psi_{2}(x_i)\right|^{2}.
\end{aligned} \tag{18}$$

The coefficients $a/2$, $a/2$, and $1-a$ of $\mathcal{S}_i$ sum to exactly 1, so applying Jensen's inequality (Lemma 3) requires them to be non-negative, which imposes the restriction $1-a\geq 0$, that is,

$$\Delta x \geq \mathcal{K}\sqrt{\Gamma(3-\alpha)}\,(\Delta t)^{\alpha/2}. \tag{19}$$

This condition is implied by (15), because $(3-2^{2-\alpha})/2 \leq 1$ for $\alpha\in(1,2]$. Under it,

$$\left|\mathcal{S}_i\right|^{2} \leq \frac{a}{2}\left|\mathcal{V}_{i-1}^{0}\right|^{2} + \frac{a}{2}\left|\mathcal{V}_{i+1}^{0}\right|^{2} + (1-a)\left|\mathcal{V}_{i}^{0}\right|^{2}.$$

Taking expectations and suprema, and using $\mathbb{E}\left|\mathcal{X}_{i}^{0}\right|^{2} = 1$ together with the independence of $\mathcal{X}_{i}^{0}$ from the deterministic initial data, we obtain

$$\begin{aligned}
&\sup_{1\leq i\leq\mathcal{N}-1}\mathbb{E}\left|\mathcal{V}_{i}^{1}\right|^{2} \leq \\
&\left[(1+\Delta t) + \frac{1}{2}\left(1+\frac{1}{\Delta t}\right)c^{2}\right]\sup_{1\leq i\leq\mathcal{N}-1}\mathbb{E}\left|\mathcal{V}_{i}^{0}\right|^{2} + 2\big(\Delta t+\Delta t^{2}\big)\sup_{1\leq i\leq\mathcal{N}-1}\left|\Psi_{2}(x_i)\right|^{2},
\end{aligned}$$

$$\mathbb{E}\left\|\mathcal{V}^{1}\right\|_{\infty}^{2} \leq \left[1+\Delta t\left(1+\frac{c^{2}}{2\Delta t}+\frac{c^{2}}{2\Delta t^{2}}\right)\right]\mathbb{E}\left\|\mathcal{V}^{0}\right\|_{\infty}^{2} + 2\big(\Delta t+\Delta t^{2}\big)\left\|\Psi_{2}\right\|_{\infty}^{2}.$$

Since

$$c^{2}/\Delta t = \sigma^{2}\Gamma(3-\alpha)^{2}(\Delta t)^{2\alpha-2}/\Delta x,$$

and

$$c^{2}/\Delta t^{2} = \sigma^{2}\Gamma(3-\alpha)^{2}(\Delta t)^{2\alpha-3}/\Delta x,$$

the bracket is bounded by $1+\lambda\Delta t$, which gives (16). $\square$

Remark 1. For $n \geq 1$, the general step (12) contains the weight $-b_{n-1} < 0$ and, in general, the weight $2b_{n-1} - b_{n-2}$, whose sign is not covered by Lemma 1. Consequently, Jensen's inequality (Lemma 3) cannot be applied to the general step, and the bounds required by Definitions 2 and 3 for all time levels are not established here. Stability over all time levels is supported numerically (Figures 1 and 2 and Table 1) and remains an open problem for an energy-type analysis.

Remark 2. If a bound with the factor $1 + \lambda\Delta t$ held at every time level, it would give $(1 + \lambda\Delta t)^n \leq e^{\lambda n\Delta t} \leq e^{\lambda\mathcal{T}}$, which is uniform in the mesh only if λ remains bounded. Under the restriction (15) alone, λ is in general unbounded as $\Delta x \to 0$; in particular, $\lambda\Delta t \to 0$ is guaranteed only when $\alpha > 4/3$. For $3/2 < \alpha \leq 2$, λ is bounded under the additional restriction

$$\Delta t^{2\alpha-3} \leq K_0\, \Delta x, \tag{20}$$

with a fixed constant $K_0 > 0$, in which case $\lambda \leq 1 + \sigma^2\Gamma(3-\alpha)^2 K_0\,(1 + \mathcal{T})$. For $\alpha = 2$, condition (20) follows from (15). For $1 < \alpha \leq 3/2$, no such uniform bound is available, and any full-time estimate would hold for each fixed mesh only.

5 Convergence Analysis

In this section, we discuss the consistency of the scheme and the error at the first time step. Convergence over all time levels requires a stability estimate for the general step, as explained in Remark 1.

Proposition 2 (One-step error estimate)**.** Let $\widehat{\mathcal{V}}_i^n$ and $\mathcal{V}_i^n$ denote the exact and approximate solutions of the TFSTWE (1) at the mesh point (x_i, t_n), respectively, and let $\mathcal{E}_i^n = \widehat{\mathcal{V}}_i^n - \mathcal{V}_i^n$. Then the error of the first step (11) of the explicit finite difference scheme satisfies

$$\mathbb{E}\,\|\mathcal{E}^1\|_\infty^2 = \mathcal{O}\big((\Delta x)^2 + \Delta t^{2-\alpha}\big)^2,$$

where $\mathbb{E}\,\|\mathcal{E}^n\|_\infty^2 := \sup_{1\leq i\leq \mathcal{N}-1} \mathbb{E}\,|\mathcal{E}_i^n|^2$.

Proof. Let $\mathcal{T}_i^n$ denote the local truncation error at time level n for $1 \leq i \leq \mathcal{N} - 1$. By the consistency of the approximations (2), (3), and (4), the local truncation errors are of order $\mathcal{O}\big((\Delta x)^2 + \Delta t^{2-\alpha}\big)$ in the mean-square sense. From Equations (11) and (12) we have, for $n = 0$,

$$\begin{aligned} \mathcal{T}_i^1 &= \widehat{\mathcal{V}}_i^1 - \frac{a}{2}\,\widehat{\mathcal{V}}_{i-1}^0 - \frac{a}{2}\,\widehat{\mathcal{V}}_{i+1}^0 - (1-a)\,\widehat{\mathcal{V}}_i^0 - \Delta t\,\Psi_2(x_i) - \frac{c}{2}\,\widehat{\mathcal{V}}_i^0\mathcal{X}_i^0 \\ &= \mathcal{O}\big((\Delta x)^2 + \Delta t^{2-\alpha}\big), \end{aligned} \tag{21}$$

and, for $n \geq 1$,

$$\begin{aligned}\mathcal{T}_i^{n+1} &= \widehat{\mathcal{V}}_i^{n+1} - a\,\widehat{\mathcal{V}}_{i-1}^{n} - a\,\widehat{\mathcal{V}}_{i+1}^{n} - (2-2a-b_1)\,\widehat{\mathcal{V}}_i^{n} - (2b_1-b_2-1)\,\widehat{\mathcal{V}}_i^{n-1}\\ &\qquad + \sum_{j=2}^{n-2}(b_{j-1}+b_{j+1}-2b_j)\,\widehat{\mathcal{V}}_i^{n-j} - (2b_{n-1}-b_{n-2})\,\widehat{\mathcal{V}}_i^{1} + b_{n-1}\,\widehat{\mathcal{V}}_i^{0} - c\,\widehat{\mathcal{V}}_i^{n}\mathcal{X}_i^{n} \qquad (22)\\ &= \mathcal{O}\big((\Delta x)^2 + \Delta t^{2-\alpha}\big).\end{aligned}$$

Subtracting the scheme (11) from (21) gives

$$\mathcal{E}_i^1 = \frac{a}{2}\,\mathcal{E}_{i-1}^0 + \frac{a}{2}\,\mathcal{E}_{i+1}^0 + (1-a)\,\mathcal{E}_i^0 + \frac{c}{2}\,\mathcal{E}_i^0\mathcal{X}_i^0 + \mathcal{T}_i^1.$$

For the exact initial condition, $\widehat{\mathcal{V}}_i^0 = \mathcal{V}_i^0$, and hence $\mathcal{E}_i^0 = 0$ for all i. Therefore $\mathcal{E}_i^1 = \mathcal{T}_i^1$, and

$$\mathbb{E}\,\big\|\mathcal{E}^1\big\|_\infty^2 = \sup_{1\le i\le \mathcal{N}-1} \mathbb{E}\,\big|\mathcal{T}_i^1\big|^2 = \mathcal{O}\big((\Delta x)^2 + \Delta t^{2-\alpha}\big)^2. \qquad \square$$

Remark 3. For $n \geq 1$, the error equation obtained by subtracting (12) from (22) contains the same negative weights as the general step. A mean-square error bound over all time levels, as required by Definition 3, therefore follows only from a stability estimate for the general step, which is not established here (see Remark 1). The observed second-order behavior for $\alpha = 2$ in Table 1 is numerical evidence for such a bound.

6 Numerical Experiments

In this section, the numerical experiments were carried out using 1000 Monte Carlo realizations to approximate the mean solution. All simulations were implemented in Python using NumPy, with the random number generator seed fixed at `np.random.seed(0)` to ensure full reproducibility of the reported results.

Example 1. Consider the TFSTWE with multiplicative space-time white noise and the following initial and boundary conditions:

$$\begin{aligned} {}^{C}\mathscr{D}_t^{\alpha}\mathcal{V}(x,t) &= \mathcal{K}^2\,\frac{\partial^2\mathcal{V}(x,t)}{\partial x^2} + \sigma\,\mathcal{V}(x,t)\,\dot{\mathcal{W}}(x,t), && (x,t)\in[0,1]\times[0,1],\ 1<\alpha\le 2,\\ \mathcal{V}(x,0) &= \sin(5\pi x) + 2\sin(7\pi x), && 0<x\le 1,\\ \mathcal{V}_t(x,0) &= 0, && 0<x\le 1,\\ \mathcal{V}(0,t) &= 0, && 0<t\le 1,\\ \mathcal{V}(1,t) &= 0, && 0<t\le 1.\end{aligned}$$

When $\alpha = 2$ and $\sigma = 0$, the exact solution of the governing equation in Example 1 is [6]

$$\mathcal{V}(x,t) = \sin(5\pi x)\cos(5\pi\mathcal{K}t) + 2\sin(7\pi x)\cos(7\pi\mathcal{K}t). \qquad (23)$$

The numerical results are shown in Figures 1–5 and Table 1 and are discussed in Section 7.

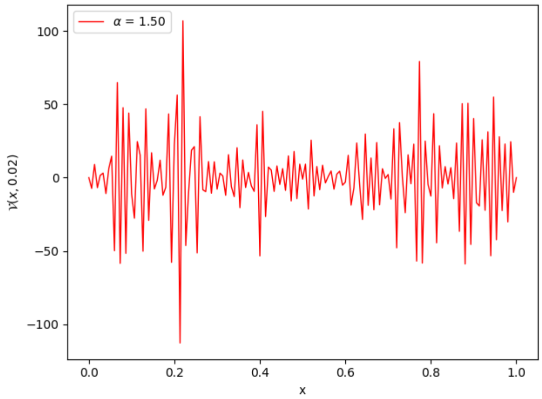

Figure 1: Unstable numerical solution of the TFSTWE for $\alpha = 1.5$ at time $t = 0.02$.

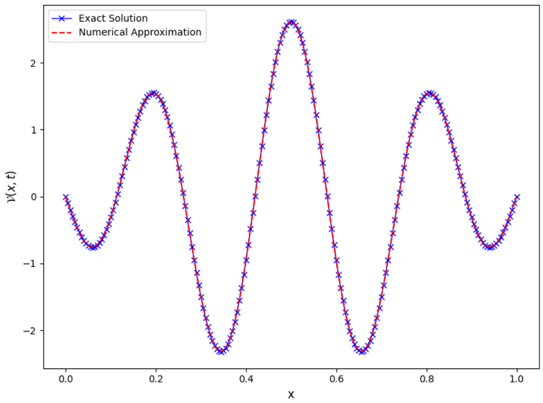

Figure 2: Comparison of the exact solution (23) and the numerical solution of the TFSTWE for $\alpha = 2$, $\sigma = 0$, and $\mathcal{K} = 1$.

Table 1: Global MSE and empirical convergence order $p = \frac{1}{2}\log_2\left(\mathrm{MSE}_{\mathrm{coarse}}/\mathrm{MSE}_{\mathrm{fine}}\right)$ across grid refinements for $\alpha = 2$, as the noise intensity σ decreases from 1 to 0.0001.

	$\Delta x = 1/50$, $\Delta t = 1/100$	$\Delta x = 1/100$, $\Delta t = 1/200$		$\Delta x = 1/200$, $\Delta t = 1/400$		$\Delta x = 1/400$, $\Delta t = 1/800$	
σ	MSE	MSE	p	MSE	p	MSE	p
1	5.787672×10^{-2}	5.338372×10^{-2}	0.058	5.253846×10^{-2}	0.012	5.246564×10^{-2}	0.001
0.1	6.475157×10^{-3}	8.926669×10^{-4}	1.429	5.383908×10^{-4}	0.365	5.348914×10^{-4}	0.005
0.01	5.976572×10^{-3}	3.802779×10^{-4}	1.987	2.869329×10^{-5}	1.864	6.815487×10^{-6}	1.037
0.001	5.972051×10^{-3}	3.750106×10^{-4}	1.997	2.359619×10^{-5}	1.996	1.530227×10^{-6}	1.974
0.0001	5.972052×10^{-3}	3.749432×10^{-4}	1.997	2.354519×10^{-5}	1.996	1.476652×10^{-6}	1.998

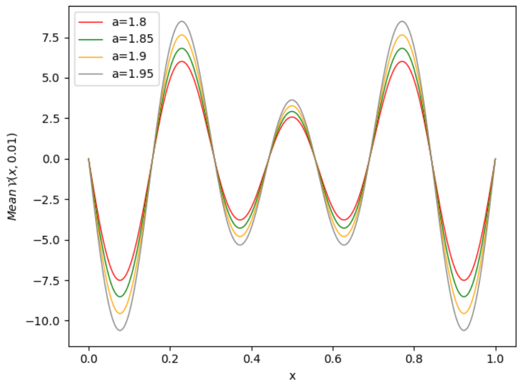

(a) $\sigma = 0$

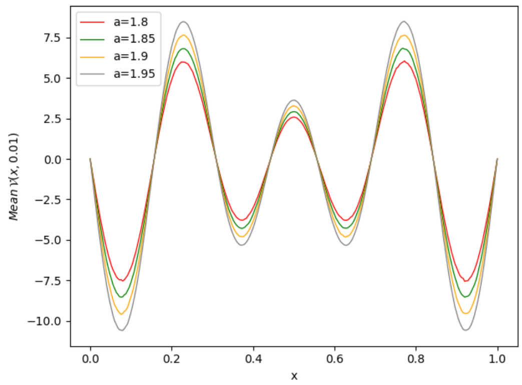

(b) $\sigma = 1$

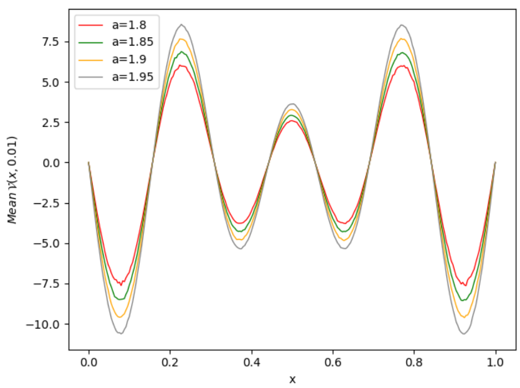

(c) $\sigma = 2$

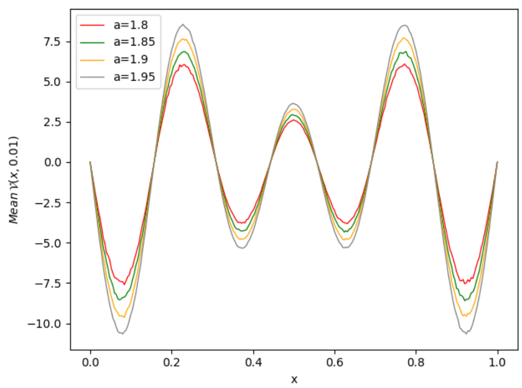

(d) $\sigma = 3$

Figure 3: Approximate two-dimensional mean solutions of the TFSTWE at time $t = 0.01$ for $\alpha = 1.8, 1.85, 1.9,$ and 1.95, with $\Delta x = 1/250$ and $\Delta t = 1/500$: (a) $\sigma = 0$, (b) $\sigma = 1$, (c) $\sigma = 2$, and (d) $\sigma = 3$.

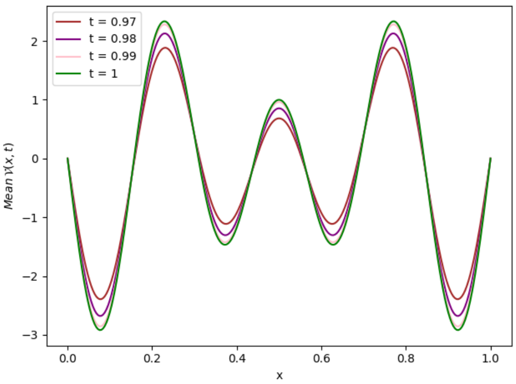

(a) $\sigma = 0$

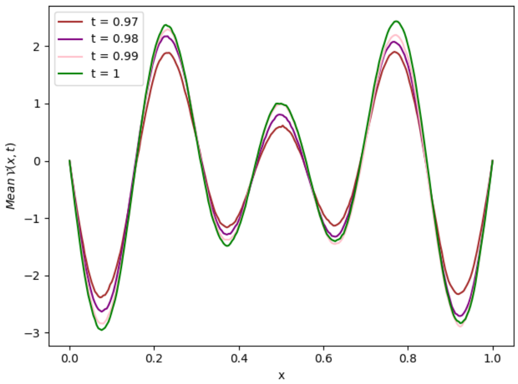

(b) $\sigma = 1$

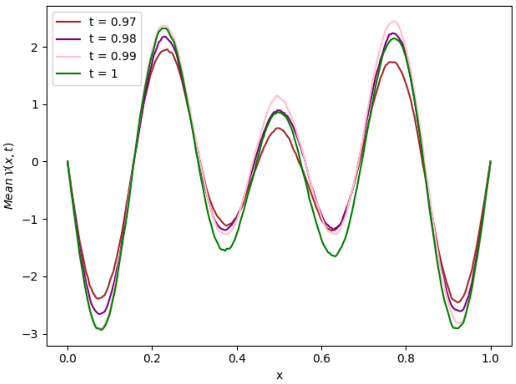

(c) $\sigma = 2$

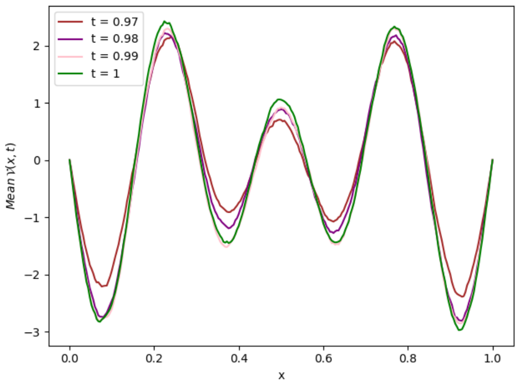

(d) $\sigma = 3$

Figure 4: Approximate two-dimensional mean solutions of the TFSTWE for $\alpha = 2$ at times $t = 0.97, 0.98, 0.99,$ and 1, with $\Delta x = 1/250$ and $\Delta t = 1/500$: (a) $\sigma = 0$, (b) $\sigma = 1$, (c) $\sigma = 2$, and (d) $\sigma = 3$.

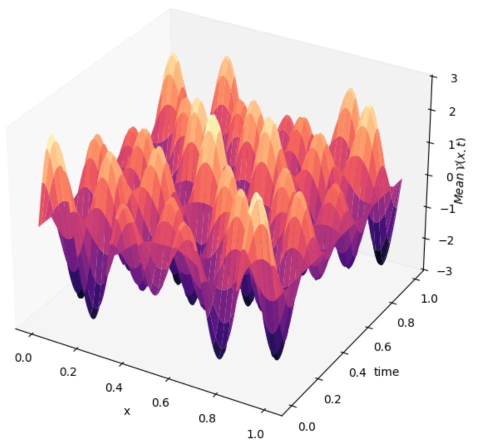

(a) $\sigma = 0$

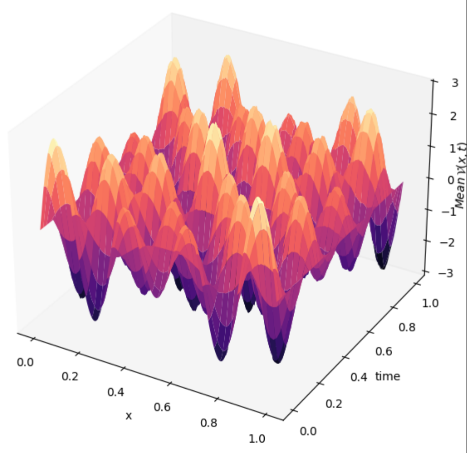

(b) $\sigma = 1$

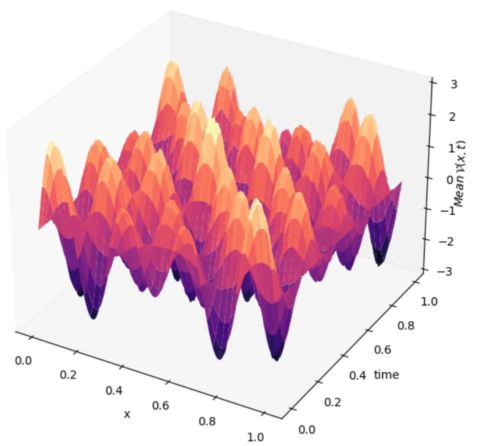

(c) $\sigma = 2$

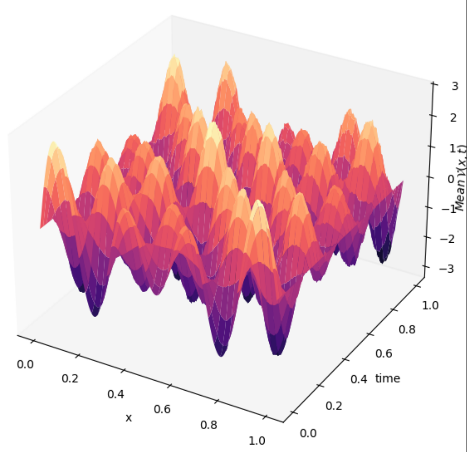

(d) $\sigma = 3$

Figure 5: Approximate three-dimensional mean solutions of the TFSTWE for $\alpha = 2$, with $\Delta x = 1/250$ and $\Delta t = 1/500$: (a) $\sigma = 0$, (b) $\sigma = 1$, (c) $\sigma = 2$, and (d) $\sigma = 3$.

7 Results and Discussion

We validate the proposed scheme for the TFSTWE using graphical representations, comparisons with the exact solution, and a global MSE analysis. When the noise intensity σ is large (specifically, $\sigma \geq 1$), the stochastic fluctuations become clearly visible in the approximate mean solution profiles. These findings collectively indicate how the dynamics of the solution are shaped simultaneously by the fractional order and the stochastic component.

To examine the efficiency of the method, we performed simulations for multiple values of the fractional order α and the noise intensity σ. Figure 1 shows the parameter regimes in which the numerical solution becomes unstable, which illustrates the need for a time-step restriction such as (15) of Proposition 1. This indicates that the explicit FDM solves the TFSTWE consistently under the given conditions. Figure 2 compares the exact solution (23) with the approximate numerical solution for $\alpha = 2$ and $\sigma = 0$, which validates the accuracy of the method.

Figures 3 and 4 further examine how the stochastic term influences the two-dimensional approximate mean solutions. Figure 3 illustrates these effects for the fractional orders $\alpha \in \{1.80, 1.85, 1.90, 1.95\}$ at the early time $t = 0.01$ and for the noise intensities $\sigma \in \{0, 1, 2, 3\}$. Figure 4 shows the solutions for $\alpha = 2$ at the final times $t = 0.97$ to $t = 1$, indicating that the noise continues to influence the system as it evolves. Finally, Figure 5 presents the three-dimensional approximate mean solutions, visualizing the computed values of $\mathcal{V}(x, t)$ for $\alpha = 2$ across varying noise intensities.

Table 1 reports the global MSE and the empirical order p for $\alpha = 2$, comparing the TFSTWE with its classical limit as σ decreases from 1 to 0.0001. For $\sigma = 0.001$ and $\sigma = 0.0001$, $p \approx 2$ at all resolutions, confirming that the TFSTWE recovers the second-order accuracy of the classical scheme as $\sigma \to 0$. As σ increases, p drops below 2, and it does so earlier: for $\sigma = 0.01$, it stays near 2 until the finest grid, whereas for $\sigma = 0.1$ and $\sigma = 1$, it falls almost immediately. This occurs because the noise adds a fixed error that does not decrease with grid refinement; once this fixed error exceeds the decreasing truncation error, further refinement no longer improves the accuracy. The MSE values reflect this pattern: on the coarsest grid, the MSE is nearly identical across all small values of σ, but on the finest grid, it varies sharply with σ. This indicates that σ determines how much refinement can help, even though the scheme itself shows second-order convergence numerically for $\alpha = 2$.

8 Conclusion

In this paper, an explicit FDM was developed to solve the TFSTWE with fractional order $\alpha \in (1, 2]$. The method incorporates multiplicative space-time white noise to simulate stochastic perturbations, and the Caputo fractional derivative accounts for memory effects. The mean approximate solutions for a particular example were plotted using Python. Increasing the noise intensity makes the wave propagation increasingly irregular and stochastically perturbed, which has a major effect on the amplitude and smoothness of the solution. For the first time step, a mean-square stability bound (Proposition 1) and an error estimate (Proposition 2) were derived; stability and convergence over all time levels are supported by the numerical experiments (Table 1) and remain to be proved (Remarks 1 and 3).

Limitations. (a) A stability and convergence proof over all time levels is not provided, because the scheme contains negative weights at later time levels, so the analysis is limited to the first step and is complemented by numerical evidence; (b) the method is restricted to one spatial dimension; (c) the error analysis does not provide strong convergence rates in the probabilistic sense (only mean-square convergence of the scheme is established); and (d) no comparison with an implicit or Crank–Nicolson analogue is provided.

Future work. (1) Extension of the explicit FDM to two-dimensional domains for the TFSTWE, where the noise approximation becomes more involved and the computational cost increases substantially; (2) development of an unconditionally stable implicit or semi-implicit scheme for the multiplicative-noise TFSTWE, building on the Crank–Nicolson approach of Mojad et al. [15] to overcome the conditional stability restriction; (3) investigation of the strong convergence rate (in the $L^2(\Omega)$ sense), rather than only the mean-square convergence of the numerical scheme, using Malliavin calculus or stochastic Gronwall arguments; and (4) application of the proposed methodology to nonlinear TFSTWEs, where multiplicative noise interacts with nonlinear wave terms arising in continuum mechanics and geophysical wave modeling.

Overall, this work offers a computationally simple framework for simulating stochastic fractional wave propagation, while identifying gaps in dimensionality, the full-time stability and convergence theory, and the stability class that future work should address.

Declarations

Availability of Supporting Data

The data that support the findings of this study are available from the corresponding author upon reasonable request.

Funding

The first author gratefully acknowledges the financial support provided by the Chhatrapati Shahu Maharaj Research, Training and Human Development Institute (SARTHI), Government of Maharashtra, for funding this research work.

Conflict of Interest

The authors declare that they have no known competing financial interests or personal relationships that could have influenced the work reported in this paper.

Author Contributions

Priti Mojad: Conceptualization; Formal Analysis; Writing – Original Draft; Writing – Review & Editing; Project Administration. **Babasaheb Gavhane**: Conceptualization; Data Curation; Writing – Review & Editing; Visualization. **Shrikisan Gaikwad**: Software and Validation; Resources; Writing – Review & Editing. **Kalyanrao Takale**: Methodology; Writing – Review & Editing; Visualization. **Chetan Shirore**: Investigation; Writing – Review & Editing; Supervision.

Artificial Intelligence Statement

Artificial intelligence (AI) tools, including large language models, were used solely for language editing and improving the readability of the manuscript. AI tools were not used to generate research ideas, perform analyses, interpret results, or produce the scientific content of the study. All scientific conclusions and intellectual contributions were made exclusively by the authors.

Publisher's Note

The publisher remains neutral regarding jurisdictional claims in published maps and institutional affiliations.

References

[1] Bayer, C., Qiu, J., Yao, Y. (2022). "Pricing options under rough volatility with backward SPDEs". *SIAM Journal on Financial Mathematics*, 13, 179–212. https://doi.org/10.1137/20M1357639

[2] Chen, L., Hu, G., Hu, Y., Hu, J. (2017). "Space-time fractional diffusions in Gaussian noisy environment". *Stochastics*, 89, 171–206. https://doi.org/10.1080/17442508.2016.1146282

[3] Chukwuyem, N. J., Nkonyeasua, N. I., Apanapudor, J. S. (2025). "Crank-Nicolson finite element method for the time fractional stochastic wave equation". *Mathematics and Statistics*, 13(3), 154–162. https://doi.org/10.13189/ms.2025.130304

[4] Darehmiraki, M. (2018). "An efficient solution for stochastic fractional partial differential equations with additive noise by a meshless method". *International Journal of Applied and Computational Mathematics*, 4, 1–13. https://doi.org/10.1007/s40819-017-0455-9

[5] Demir, I. (2025). "Refinements of the Jensen inequality and estimates of the Jensen gap based on interval-valued functions". *Mathematical Methods in the Applied Sciences*, 48, 12567–12576. https://doi.org/10.1002/mma.11046

[6] Ghode, K., Takale, K., Gaikwad, S. (2021). "New technique for solving time fractional wave equation: Python". *Journal of Mathematical and Computational Science*, 11, 5327–5343. https://www.scik.org/index.php/jmcs/article/view/6048

[7] Goufo, F. D., Nieto, J. J. (2018). "Attractors for fractional differential problems of transition to turbulent flows". *Journal of Computational and Applied Mathematics*, 339, 329–342. https://doi.org/10.1016/j.cam.2017.08.026

[8] Hoult, J., Yan, Y. (2024). "Numerical approximation for a stochastic fractional differential equation driven by integrated multiplicative noise". *Mathematics*, 12(3), Art. no. 365. https://doi.org/10.3390/math12030365

[9] Kilbas, A. A., Srivastava, H. M., Trujillo, J. J. (2006). *Theory and applications of fractional differential equations*. North-Holland Mathematics Studies, 204. Amsterdam: Elsevier.

[10] Li, J., Zhang, J., Jiang, Y. (2025). "A finite difference method for Caputo generalized time fractional diffusion equations". *Fractal and Fractional*, 10, Art. no. 19. https://doi.org/10.3390/fractalfract10010019

[11] Ma, J., Ogunsolu, M., Qiu, J., Sezer, D. (2023). "Credit risk pricing in a consumption-based equilibrium framework with incomplete accounting information". *Mathematical Finance*, 33, 666–708. https://doi.org/10.1111/mafi.12386

[12] Mirzaee, F., Samadyar, N. (2020). "Combination of finite difference method and meshless method based on radial basis functions to solve fractional stochastic advection–diffusion equations". *Engineering with Computers*, 36, 1673–1686. https://doi.org/10.1007/s00366-019-00789-y

[13] Mirzaee, F., Sayevand, K., Rezaei, S., Samadyar, N. (2021). "Finite difference and spline approximation for solving fractional stochastic advection-diffusion equation". *Iranian Journal of Science and Technology, Transactions A: Science*, 45, 607–617. https://doi.org/10.1007/s40995-020-01036-6

[14] Moghaddam, B. P., Babaei, A., Dabiri, A., Galhano, A. (2024). "Fractional stochastic partial differential equations: Numerical advances and practical applications—A state of the art review". *Symmetry*, 16, Art. no. 563. https://doi.org/10.3390/sym16050563

[15] Mojad, P., Gavhane, B., Gaikwad, S., Takale, K. (2025). "Crank-Nicolson approximation to space-time fractional stochastic traveling wave equation with additive white noise". *Boletim da Sociedade Paranaense de Matemática*, 43, 1–15. https://doi.org/10.5269/bspm.77257

[16] Roth, C. H. (2002). "Difference methods for stochastic partial differential equations". *ZAMM Journal of Applied Mathematics and Mechanics*, 82, 821–830. https://doi.org/10.1002/1521-4001(200211)82:11/12<821::AID-ZAMM821>3.0.CO;2-L

[17] Sababheh, M., Choi, D. (2016). "A complete refinement of Young's inequality". *Journal of Mathematical Analysis and Applications*, 440(1), 379–393. https://doi.org/10.1016/j.jmaa.2016.03.049

[18] Singh, A. K., Mehra, M. (2023). "Difference methods for stochastic space fractional diffusion equation driven by additive space–time white noise via Wong–Zakai approximation". *Journal of Mathematical Chemistry*, 61, 47–74. https://doi.org/10.1007/s10910-022-01408-w

[19] Singh, S., Singh, S., Aggarwal, A. (2023). "A new spline technique for the time fractional diffusion-wave equation". *MethodsX*, 10, Art. no. 102007. https://doi.org/10.1016/j.mex.2023.102007

[20] Song, E. (2023). "Impact of noise on the instability of spiral waves in stochastic 2D mathematical models of human atrial fibrillation". *Journal of Biological Physics*, 49, 521–533. https://doi.org/10.1007/s10867-023-09644-0

[21] Song, J., Song, X., Xu, F. (2020). "Fractional stochastic wave equation driven by Gaussian noise rough in space". *Bernoulli*, 26(4), 2699–2726. https://doi.org/10.3150/20-BEJ1204

[22] Sun, Z., Wu, X. (2006). "A fully discrete difference scheme for a diffusion-wave system". *Applied Numerical Mathematics*, 56(2), 193–209. https://doi.org/10.1016/j.apnum.2005.03.003

[23] Week, B., Nuismer, S. L., Harmon, L. J., Krone, S. M. (2021). "A white noise approach to evolutionary ecology". *Journal of Theoretical Biology*, 521, Art. no. 110660. https://doi.org/10.1016/j.jtbi.2021.110660

[24] Zhang, Z., Karniadakis, G. E. (2017). "Numerical methods for stochastic partial differential equations with white noise". *Applied Mathematical Sciences*, 196. https://doi.org/10.1007/978-3-319-57511-7

Authors' Bio-sketches

Priti Mojad is affiliated with the Department of Mathematics, New Arts Commerce and Science College, Ahmednagar, India (affiliated to Savitribai Phule Pune University, Pune). Her research interests include fractional stochastic differential equations, numerical methods, and finite difference schemes.

Babasaheb Gavhane is affiliated with the Department of Mathematics, K. J. Somaiya College of Arts, Commerce and Science, Kopargaon, India. His research interests include fractional stochastic differential equations, fractional differential equations, numerical methods.

Shrikisan Gaikwad is affiliated with the Department of Mathematics, New Arts Commerce and Science College, Ahmednagar, India. His research interests include fractional differential equations, numerical methods, and Python-based scientific computing.

Kalyanrao Takale is affiliated with the Department of Computer Science, Jaykranti College of Computer Science and Management, Pune, India. His research interests include fractional differential equations, the Adomian decomposition method, and fractional stochastic differential equations.

Chetan Shirore is affiliated with the Department of Mathematics, K.R.T. Arts, B.H. Commerce and A.M. Science College, Nashik, India. His research interests include numerical methods for fractional stochastic equations and computational tools for mathematical typesetting. Corresponding author. Email: chetanshirore@kthmcollege.ac.in.